2 CHARACTERISTICS OF SOME HIGH TITANIA SLAGS PRODUCED IN A 3 MVA PLASMA FURNACE

2.1 INTRODUCTION

The smelting of ilmenite requires fine control of the smelting process in order to produce an acceptable slag product on a consistent basis. This section will deal with some of the characteristics of the slag product. The aims of this section of the study are as follows:

- By improving our understanding of the slag product, and the factors relevant in the production of the liquid slag, it will lead to improvements in the smelting process. In order to do this the following aspects, and the relationships between these aspects, were investigated:
  - The chemistry of the slags,
  - The tapping temperatures of the slags. This was compared to the available liquidus temperature data.
- The second aim of this section is to gain an understanding of the mineralogy and chemistry of solidified titania slag. In the next chapter the decrepitation behaviour of titania slags will be investigated. This section is to provide a basis for comparing decrepitated slag with slag that did not decrepitate.

2.2 LITERATURE SURVEY

2.2.1 MINERALOGY OF HIGH TITANIA SLAGS

According to Russian investigators as quoted by Handfield and Charette (1971) the main constituents found in industrial high titania slags in the solid state were as follows:

- A solid solution of the anosovite group (orthorhombic crystal structure). The following general formula was proposed to take into account the extensive solid solution:

$$m[(Ti, Mg, Mn, Fe)O.2TiO_2].n[(Ti, Fe, Al, Cr, V)_2O_3.TiO_2]$$

  According to this formula, iron can potentially be present as Fe^{2+} and Fe^{3+}, while titanium can potentially be present as Ti^{2+}, Ti^{3+} and Ti^{4+}.
- Minerals based on a solid solution having the Ti_2O_3 type of structure (rhombohedral). The following general formula was proposed to take into account the extensive solid solution:

$$a[(Ti, Mg, Mn, Fe)O.TiO_2].b[(Ti, Al, Cr, V, Fe)_2O_3]$$

  According to this formula, iron can potentially be present as Fe^{2+} and Fe^{3+}, while titanium can potentially be present as Ti^{2+}, Ti^{3+} and Ti^{4+}.
- The third phase consisted of glassy material with complex compositions.

For the titaniferous portion of the slags, the mutual dissolution of the elements to form a wide region of solid solutions is explained by the ionic radii of the constituent elements. This can also be explained by the small difference (in most cases less than 5 per cent) in the lattice constants of the end member phases of the solid solutions. The close ionic radii of

the cations can be seen by comparing the data of the relevant cations in Table 2 (data from Huheey, 1983). A comparison of the data for iron, manganese and magnesium illustrates this.

Table 2: Effective ionic radii of elements relevant to ilmenite smelting (Huheey, 1983)

Cation	Coordination number	Radius (Å)	Cation	Coordination number	Radius (Å)
Al^{3+}	4	0.53	Mn^{2+}	4	0.80 (HS)
Al^{3+}	6	0.675	Mn^{2+}	6	0.97 (HS)
Ca^{2+}	6	1.14	Mn^{2+}	8	1.10
Ca^{2+}	8	1.26	Si^{4+}	4	0.40
Cr^{2+}	6	0.94 (HS)	Si^{4+}	6	0.54
Cr^{3+}	6	0.755	Ti^{2+}	6	1.00
Fe^{2+}	4	0.77 (HS)	Ti^{3+}	6	0.81
Fe^{2+}	6	0.92 (HS)	Ti^{4+}	4	0.56
Fe^{2+}	8	1.06 (HS)	Ti^{4+}	6	0.745
Fe^{3+}	4	0.63 (HS)	Ti^{4+}	8	0.88
Fe^{3+}	6	0.785 (HS)	V^{3+}	6	0.78
Mg^{2+}	4	0.71	Zr^{4+}	4	0.73
Mg^{2+}	6	0.86	Zr^{4+}	6	0.86
Mg^{2+}	8	1.03	Zr^{4+}	8	0.98

HS – High spin

Handfield and Charette (1971) also discussed work carried out by previous investigators on Sorel slags. It was concluded that the main constituents in these slags were $RO.2TiO_2$ (R = Mg^{2+}, Fe^{2+} and Ti^{2+}) and $R_2O_3.TiO_2$ (R = Fe^{3+}, Al^{3+} and Ti^{3+}) phases. The opinion was expressed that these compounds are soluble in each other in all proportions and that the largest portion of the slag is a solid solution of the above compositions. It was also stated that the siliceous portion of the slag was composed of feldspathic materials (anorthite, albite and orthoclase) and mixed metasilicates of iron calcium and magnesium. A large portion of this is in a glassy state.

Handfield and Charette (1971) also concluded that melting high titania slags does not change their short range order significantly. High titania slags are also structurally different from the polymerizing silicate melts. According to Sommerville and Bell (1982) TiO_6^{8-} is the most likely ions to be present in titania slags. The reasons given for this is the clear preference of Ti^{4+} for octahedral co-ordination (compared to tetrahedral co-ordination for Si^{4+}), the observed viscosity data for high titania slags (discussed later), crystallisation characteristics and the structure of solid anosovite.

Toromanoff and Habashi (1984) investigated the mineralogical composition of a typical titanium slag from Sorel. Based on X-ray diffraction and microprobe analyses the slag was found to consist mainly of an iron magnesium titanate, armalcolite. The crystals were

cemented together by a calcium aluminium silicate phase. Trace amounts of rutile were also identified.

Also present were a small number of large metallic iron globules, some of them having a rim consisting of ferrous sulphide. These globules varied in size between 15 and 150 μm. It was assumed that these globules originated from the metal produced in the electric furnace, and were entrained in the slag during settling. Numerous small iron globules, 1 to 2 μm in size, were also observed in the slag. Because of their smaller size it was postulated that these globules had a different origin than the larger globules. The following reaction was proposed as a mechanism for the formation of the small metallic globules:

$$2Ti^{3+} + Fe^{2+} = 2Ti^{4+} + Fe^{0} \ldots (H)$$

This reaction was shown to be thermodynamically feasible.

Borowiec (1991) used a high titania slag at Tyssedal in Norway to study the sulphidisation of the solid slag. The aim of this study was to investigate the removal of impurities by this technique. Of relevance to this study are the results reported on the microprobe analyses of the phases contained in the Tyssedal slag. These results, together with the bulk analysis of the Tyssedal slag are shown in Table 3. When compared to the bulk analysis of the slag it was calculated that the slag consisted of about 88 per cent M_3O_5 phase and 12 per cent glassy silicate phase. It should be pointed out that the Tyssedal slag was made from hard rock ilmenite deposits containing high levels of impurities such as MgO, SiO_2 and Al_2O_3. The slags used in this study was obtained by the smelting of beach sand ilmenite deposists in which the impurity levels are significantly lower.

Table 3: Bulk and phase analyses of Tyssedal slag (Borowiec, 1991).

Components	Bulk analysis (mass %)	Microprobe analyses (mass %)	
		M_3O_5 phase	Glassy silicate matrix
TiO_2	75.0	64.92	11.74
Ti_2O_3	-	17.45	-
FeO	7.6	7.38	8.96
SiO_2	5.3	0.02	44.62
Al_2O_3	2.3	1.80	5.72
MgO	7.9	7.50	10.62
MnO	0.4	0.27	1.55
CaO	0.6	0.01	13.87
V_2O_3	0.52	0.60	0.06
Cr_2O_3	0.01	0.01	-

Reznichenko et. al. (1981) investigated metallic inclusions that form in high titania slags produced in Russia. Samples were taken from slag ingots that were quenched in water. These slags contained between 2 and 7.5 per cent ferrous oxide. The metal inclusions consist of two phases; metal and sulphide. A sulphide shell rim generally surrounds the metal phase, with the larger buttons containing rounded or irregular-shaped sulphide inclusions. The chemical composition for the sulphide phases was 55 to 70 per cent iron, 3 to 5 per cent manganese and 35 to 40 per cent sulphur. The authors suggest that sulphur,

introduced via the feed, has an outer electron shell similar to that of oxygen. As in the case of oxygen it can also form octahedral complexes with the iron cation. Because of the similarity of their electronic structure and the small difference in size complex oxy-sulphide compounds can form in the melt. These compounds are of the type $[FeO_xS_y]^n$, where x + y = 6. On cooling these compounds decompose to form a two-phase button as described above. It was also suggested that pure metallic iron is formed according to reaction (I), with mineralogical analysis confirming the occurrence of this reaction in the solid stage of the process. This is the same as reaction (H), except that it is written in compounds rather than ions. As the temperature decreases, ΔG^0 becomes more negative. This results in the reaction becoming thermodynamically more favourable, shifting more towards the formation of metallic iron.

$$3Ti_2O_3 + FeO = Fe^0 + 2Ti_3O_5 \ldots (I)$$

$$\Delta G^0 = -\ 110\ 667 + 19.874T \text{ (J, 700 to 1642 K)}$$

Various investigators studied the solid solution series depicted as M_3O_5, where M can be a combination of a wide number of cations. Information regarding this M_3O_5 solid solution series is relevant to this study, as M_3O_5 phases of various compositions have been identified as the main phase present in high titania slags (Toromanoff and Habashi, 1984; Borowiec, 1991). It has been shown that the M_3O_5 phase has a pseudobrookite structure, AB_2O_5 (see for example Grey and Ward, 1973; Wechsler et. al., 1976; Brown and Navrotsky, 1989). A and B represent two symmetrically distinct, octahedral cation sites within this structure, with 4 A and 8 B sites within the unit cell. The A site in general is larger and more distorted than the B site.

Grey and Ward (1973) studied the solid solution series $FeTi_2O_5$-Ti_3O_5 as a function of temperature and oxygen partial pressure. From X-ray diffraction studies they found that the solid solution is complete at temperatures above 1350 °C. For the series $Fe_xTi_{3-x}O_5$ (with $0 \leq x \leq 1$) it was found that with $x > 0.35$ the compounds had an orthorhombic pseudobrookite structure. With $x < 0.35$ the compounds had a monoclinic distortion of this structure, with the distortion increasing towards the Ti_3O_5 composition. They also reported that for $FeTi_2O_5$ approximately 72 per cent of the Fe^{2+} is found at the A site. This increases slightly to 75 per cent at a composition of $Fe_{0.75}Ti_{2.25}O_5$. For compositions close to Ti_3O_5 this value drops to approximately 60 per cent.

Eriksson et. al. (1996) compiled the Ti_3O_5-$FeTi_2O_5$ phase diagram shown in Figure 5. This shows that the Ti_3O_5-$FeTi_2O_5$ solid solution is continuous only at temperatures above approximately 1350 °C under equilibrium conditions (in agreement with the study of Grey and Ward (1973) mentioned above). The structure change at x = 0.35 is also shown.

Bowles (1988) made a summary of the site occupancies of various pseudobrookite phases. This is shown in Table 4. From this it can be seen that Fe^{2+} is concentrated in the A site, with Ti^{4+} concentrated in the B site. For Ti_3O_5 the Ti^{3+} cation mostly fills the A site, with only a small portion of the A site filled by Ti^{4+}. The series from pseudobrookite to Ti_3O_5 represents a steady replacement of Fe by Ti, with reduction first of Fe^{3+} to Fe^{2+} and then some of the Ti^{4+} to Ti^{3+}. It was also noted by Bowles (1988) that a large number of naturally occurring minerals of the pseudobrookite structure occurs.

Teller et. al. (1990, pp. 334-350) made a structural analysis of several pseudobrookite ferrous titanium oxides using neutron diffraction and Mössbauer spectroscopy techniques. Under reducing conditions it was possible to quench synthetic metastable materials that contain Fe^{2+} and Ti^{3+} cations within the same oxide lattice. These materials are thermodynamically unstable at room temperature with respect to Fe^{0} and Ti^{4+} (see reactions (H) and (I)). Two materials (approximating $FeTi_2O_5$ and $Fe_{0.5}Mg_{0.5}Ti_2O_5$) were prepared at 1200 °C, where the reducing conditions were strictly controlled. In addition two slags samples at temperatures greater than 1700 °C were prepared by the reduction of ilmenite with carbon. The stoichiometries of these samples were $Ti_{2.52}Fe_{0.33}Mn_{0.05}O_5$ and $Ti_{2.36}Fe_{0.33}Mg_{0.31}O_5$ respectively. It was found that the temperature of preparation and the conditions of reduction largely determined the distribution of the cations in the pseudobrookite stucture. For the samples prepared at 1200 °C it was found that Fe^{2+} was distributed between both the A and B sites. For the samples prepared at 1700 °C it was found that Fe^{2+} reported exclusively to the A site. These results are shown in Table 5. It was concluded that a "disordered" model best described the low temperature structures. It was also found that the Mg and Fe occupancies of the A and B sites were not identical.

Figure 5: Phase diagram of the $FeTi_2O_5$-Ti_3O_5 join (Eriksson et. al., 1996)

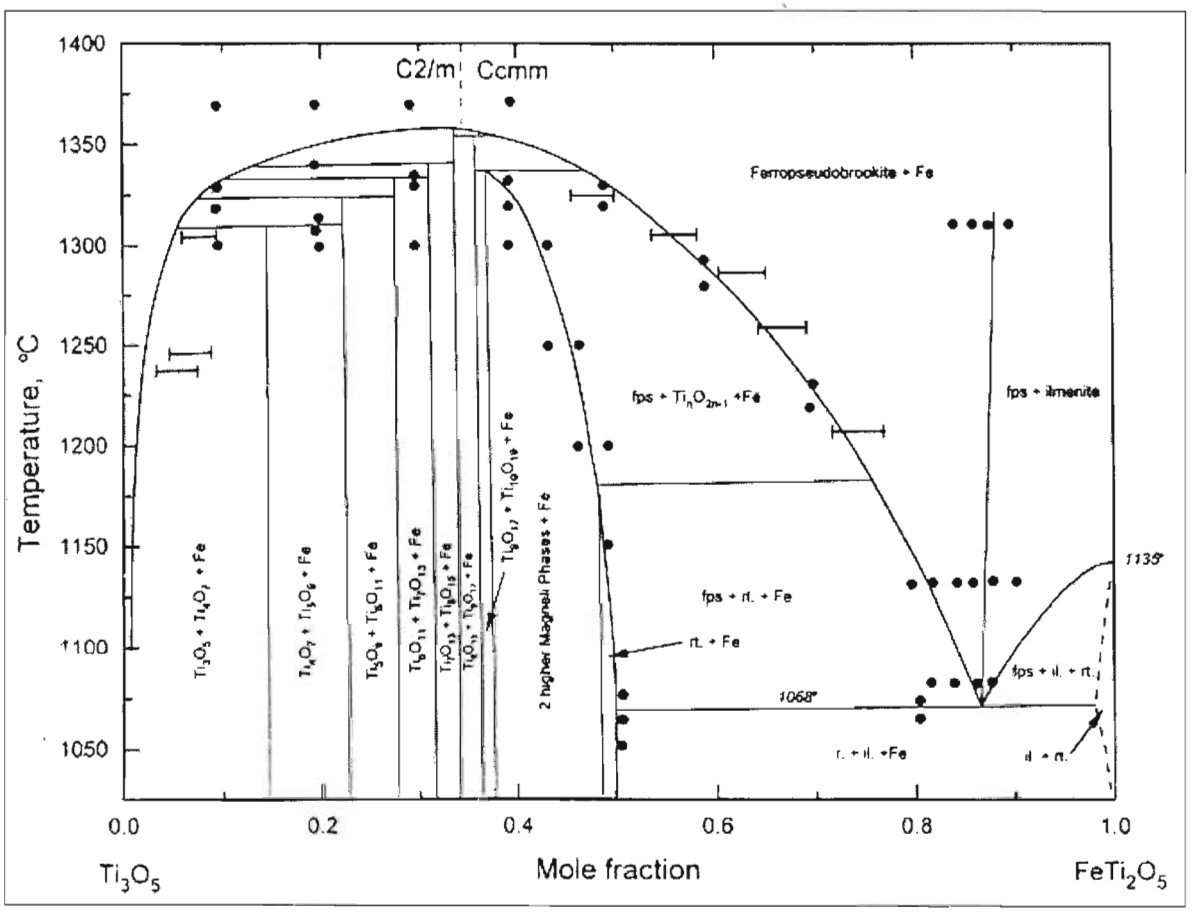

X-ray diffraction data for various samples are given in Table 6. This shows that the major peaks are found at d values of approximately 3.50 and 2.76 Å. The chemical composition of the lunar armalcolite and the Sorel slag is given in Table 7.

The unit cell parameters of various M_3O_5 samples are given in Table 8. As discussed previously Grey and Ward (1973) found in their study that the orthorhombic pseudobrookite cell transforms to a monoclinic cell at a composition of approximately $Fe_{0.35}Ti_{2.65}O_5$. This monoclinic distortion increases with increasing titanium content towards Ti_3O_5. Grey and Ward (1973) also found a slight increase in the unit cell volume (0.5 per cent) from $FeTi_2O_5$ to Ti_3O_5. The a and b parameters in their results increased towards Ti_3O_5, while the c parameter decreased. Grey and Ward (1973) believed that this occurred due to increased metal-metal bonding between Ti^{3+} cations as the amount of Ti_3O_5 is increased.

Table 4: Cation distributions in various pseudobrookite phases (Bowles, 1988)

Phase	Cations in A site	Cations in B site	Reference
$FeTi_2O_5$	$Fe^{2+}_{0.68}\ Ti^{4+}_{0.32}$	$Fe^{2+}_{0.32}\ Ti^{4+}_{1.68}$	Virgo and Huggins (1975)
$FeTi_2O_5$	$Fe^{2+}_{0.72}\ Ti^{4+}_{0.28}$	$Fe^{2+}_{0.28}\ Ti^{4+}_{1.72}$	Grey and Ward (1973)
$FeTi_2O_5$	$Fe^{2+}_{0.81}\ Ti^{4+}_{0.19}$	$Fe^{2+}_{0.19}\ Ti^{4+}_{1.81}$	Navrotsky (1975)
Ti_3O_5	$Ti^{4+}_{0.05}\ Ti^{3+}_{0.95}$	$Ti^{4+}_{0.95}\ Ti^{3+}_{1.05}$	Navrotsky (1975)

Table 5: Cation distributions for various pseudobrookite samples (Teller et. al., 1990, pp.334-350)

Sample	Cations in A site	Cations in B site
$Fe_{0.93}Ti_{2.07}O_5$	$Fe_{0.70}Ti_{0.30}$	$Fe_{0.23}Ti_{1.77}$
$Fe_{0.6}Mg_{0.6}Ti_{1.8}O_5$	$Fe_{0.5}Ti_{0.5}$	$Mg_{0.6}Fe_{0.1}Ti_{1.3}$
$Ti_{2.52}Fe_{0.33}Mn_{0.05}O_5$	$Mn_{0.05}Fe_{0.33}Ti_{0.52}$	$Ti_{2.00}$
$Ti_{2.36}Fe_{0.33}Mg_{0.31}O_5$	$Mg_{0.21}Fe_{0.33}Ti_{0.46}$	$Ti_{1.90}Mg_{0.10}$

2.2.2 CHEMICAL ANALYSES OF HIGH TITANIA SLAGS

A summary of selected high titania slag analyses is shown in Table 9. Also shown are the specifications required by the two pigment manufacturing processes. As can be seen the quality of the slag products differs significantly, with only RBM and Namakwa sands producing slag containing more than 85 per TiO_2 (total Ti expressed as TiO_2). This is mainly due to the high impurity levels of the ilmenite used by the other producers. Generally chloride grade feedstocks require high levels of TiO_2 (Fisher, 1997). This is because the high temperature chlorination reactions that occur are not selective, and most of the metal oxides contained in the feed are converted to chlorides. Intermediate processes can be used to upgrade the quality of the slag. An example of this is the UGS (Upgraded Slag) product made from Sorel slag (Fisher, 1997). In this product the undesirable alkaline elements and most of the iron oxide are selectively removed. This results in a slag product with physical and chemical properties similar to natural rutile.

Table 6: X-ray diffraction data for various M_3O_5 compounds (only peaks with I/I_0 > 10)

Anderson et. al. (1970)				Toromanoff and Habashi (1984)	
Synthetic armalcolite ($Fe_{0.5}Mg_{0.5}Ti_2O_5$)		Lunar armalcolite		Sorel slag	
d values (obs.) (Å)	I/I_0	d values (obs.) (Å)	I/I_0	d values (obs.) (Å)	I/I_0
5.019	40			5.02	20
4.879	80			4.88	30
3.493	100	3.468	100	3.50	100
2.762	80	2.763	25	2.76	60
2.452	10	2.454	25	2.45	12
2.438	5			2.44	9
2.415	10	2.414	10	2.41	13
2.233	15	2.235	15	2.23	11
		2.199	15	2.19	12
				2.19	11
1.972	17	1.958	80	1.97	10
				1.96	10
				1.87	40
				1.86	12
		1.751	10		
1.675	10	1.669	10		
1.634	28	1.632	10		
1.625	13				
1.549	18			1.55	13

Table 7: Composition of lunar armalcolite and Sorel slag samples used for X-ray diffraction analyses (see Table 6)

	Analyses (mass %)	
	Lunar armalcolite (Microprobe)	Sorel slag (Bulk analyses)
TiO_2	73.4	70-72
Al_2O_3	1.62	4-6
Cr_2O_3	2.15	< 0.25
FeO	15.3	12-15
MnO	0.08	0.2-0.3
MgO	7.70	4.5-5.5
CaO	0.01	< 1.2
V_2O_3	< 0.5	0.5-0.6
SiO_2	-	3.5-5

Table 8: Unit cell data for various M_3O_5 compounds

	Teller et. al. (1990, pp. 334-350)				Grey and Ward (1973)			Anderson et. al. (1970)	
	Samples at 1200 °C	Samples at 1200 °C	Samples at > 1700 °C	Samples at > 1700 °C	-	-	-	Synthetic armalcolite	Lunar armalcolite
	$FeTi_2O_5$	$Fe_{0.5}Mg_{0.5}Ti_2O_5$	$Ti_{2.36}Fe_{0.33}Mg_{0.31}O_5$	$Ti_{2.52}Fe_{0.33}Mn_{0.05}O_5$	$FeTi_2O_5$	$Fe_{0.50}Ti_{2.50}O_5$	$Fe_{0.32}Ti_{2.68}O_5$	$Fe_{0.5}Mg_{0.5}Ti_2O_5$	See table
a (Å)	3.7498	3.7413	3.7629	3.7828	9.790	9.798	9.823	9.752 ± 0.003	9.743 ± 0.03
b (Å)	9.8057	9.7659	9.7556	9.7938	3.757	3.781	3.785	10.048 ± 0.003	10.024 ± 0.02
c (Å)	10.0675	9.9946	10.0151	10.0280	10.079	10.020	10.000	3.736 ± 0.004	3.738 ± 0.03
Cell Vol. ($Å^3$)	370.17	365.17	367.65	371.52	370.7	371.2	371.8	366.071 ± 0.322	365.077 ± 0.619

Table 9 : Chemical analyses of various high titania slags

Compound	Analyses of various slag products (mass %)					Typical specifications for chloride grade slag[e,f]	Typical specifications for sulphate grade slag[e]
	Sorel slag[a]	Sorel slag[b]	Namakwa[a] sands	RBM[a]	Tinfos[c,d]		
Total Ti as TiO_2	77.5	71.5	86.0	85.5	75		
TiO_2	-	62.1	54.9	54.3	-		
Ti_2O_3	-	8.5	28.0	28.10	-		
FeO	10.9	11.4	10.0	10.50	7.6	Minimum	
Fe^0	-	0.8	-	-	-		
Al_2O_3	3.5	4.5	1.80	1.10	1.2 to 2.3	< 2.0	
SiO_2	3.0	4.2	1.80	1.20	5.3	$SiO_2 + ZrO_2 < 2.0$	
CaO	0.6	0.7	0.16	0.16	0.6	< 0.20 to 0.25	
MgO	5.3	5.1	0.85	1.00	7.9	< 1.0	
MnO	0.2	0.2	1.50	1.80	0.4	< 2.0	
V_2O_5	0.3	0.57	0.42	0.40	0.63	< 0.4	
Cr_2O_3	0.17	0.19	0.07	0.18	0.01 to 0.09	< 0.2	
ZrO_2	-	-	0.28	-	-		
P_2O_5	-	0.03	-	-	-		< 0.05
C	-	0.02	-	-	-		
S	-	0.06	-	-	-		

a – Pesl (1997)
b - Toromanoff and Habashi (1984)
c – Skillen (1992)
d - Borowiec (1991)
e – Stanaway (1994)
f - Battle et. al. (1993)

Other properties of high titania slags, apart from the chemical composition, also play a role in the selecting the final product for the appropriate processing technology. One such aspect is the size distribution of the slag. This will be discussed in more detail in the section on the decrepitation of the titania slags.

The following reasons for the chemical specifications for the chloride process have been given (Stanaway, 1994; Battle et. al., 1993; Fisher, 1997):

- For the chloride process route CaO can cause sticking in the fluidized bed. This is also the case for MgO and MnO, although to a lesser extent. The chlorides of these elements are liquid at the chlorination temperatures and can defluidize the bed and also cause clogging in the bed.
- The operating temperature in the typical fluidized bed is too low to convert all the silica to the chloride. The silica therefore remains in the fluidized bed, accumulating and thereby reducing the throughput. Low levels of silica are therefore specified.
- A low iron content is required to minimize iron chloride disposal problems, optimize plant capacity and minimize chlorine consumption.
- Low levels of vanadium and chromium are required due to potential toxicity problems in the iron chloride waste.
- Low tin and arsenic levels are required as these elements accumulate with the titanium chloride stream.
- Uranium, thorium and other radioactive substances concentrate in some of the waste and process streams, and are therefore undesirable.

Reasons listed for the chemical specifications for the sulphate process are the following (Stanaway, 1994; Fisher, 1997):

- A low iron content is preferable in order to minimize waste disposal, optimize plant capacity and minimize reagent consumption. Some ferric iron gives an undesirable colour to the pigment product. Some ferrous iron is however required for optimum titanium dioxide crystal formation during the precipitation stage.
- Low chromium and vanadium contents are required as these elements can colour the pigment above certain levels. These elements also cause toxicity and waste disposable problems when present in the waste products.
- High calcium and phosphate levels can hinder crystal development.
- Niobium also imparts colour to the pigment.
- Uranium, thorium and other radioactive substances concentrates in some of the waste and process streams, and once again are therefore undesirable.
- The amount of Ti^{3+} in the feed needs to be limited as this forms a Ti_2O_3 product. This Ti_2O_3 product is considered to be part of the waste materials.

For the sulphate processing route feedstocks in which the iron is in the divalent state and titanium in the tetravalent state is preferred. Ferric iron must be avoided, since these ions adsorb on the surface of the TiO_2 particles in the digestion solution and discolour the TiO_2 (Fisher, 1997). Ferric iron in the feedstock is usually reduced by the addition of iron scrap at additional cost.

As previously explained, ilmenite is reduced with a carbonaceous reductant during the reduction process. During this process most of the iron is reduced to metal, while some of the titanium is reduced from the tetravalent to the trivalent state. Increasing the reductant addition in the ilmenite smelting process, with the required energy input, decreases the iron oxide

content in the slag and increases the amount of trivalent titanium present in the slag. Based on testwork in a 150 kVA pilot furnace, Grau and Poggi (1978) illustrated the relationship between the TiO_2, Ti_2O_3 and FeO content of Sorel slag. This is shown in Figure 6, with the equivalent per cent TiO_2 being the total titanium content expressed as titanium dioxide. The relationship between the Ti_2O_3 and FeO contents was determined from the data shown in Figure 6 (data set used for calculation shown in Appendix A) and is expressed by the linear regression equation (I):

$$\% Ti_2O_3 = -(1.49)(\% FeO) + 37.17 \; ; R^2 = 0.74 \ldots (I)$$

Figure 6 : Variations in the FeO and Ti_2O_3 content of Sorel slags (Grau and Poggi, 1978)

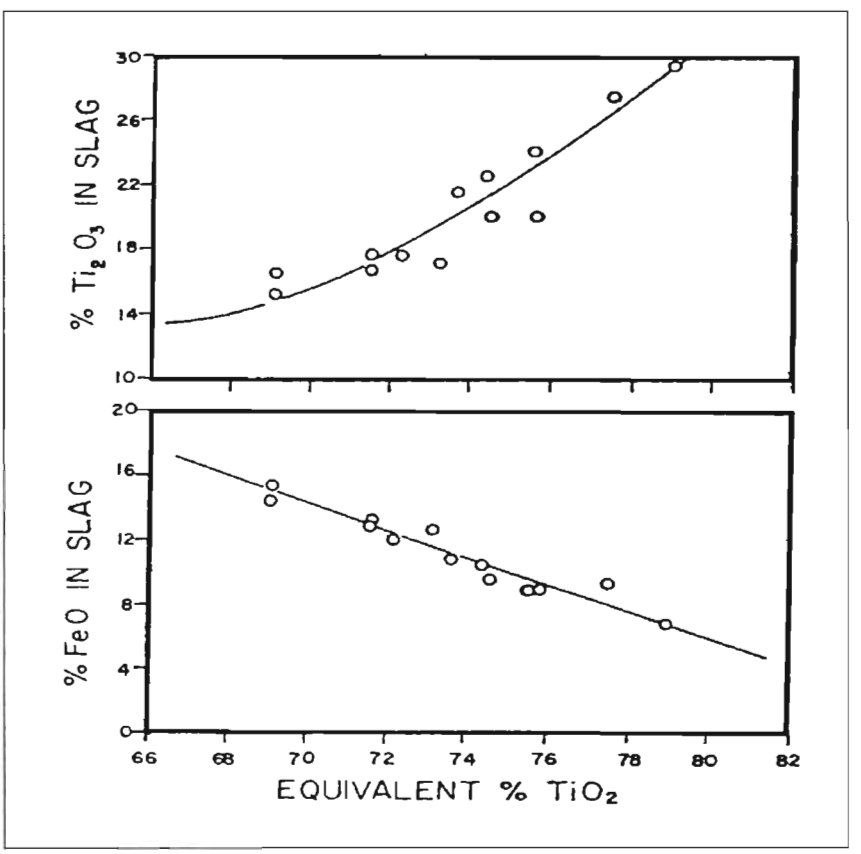

Ban (1988) investigated the smelting of Quilon ilmenite (concentrate from India) in a DC furnace. The ilmenite contained 60 per cent TiO_2 and 32.4 per cent FeO. The main impurities in the ilmenite were Al_2O_3 (1.6 per cent) and SiO_2 (0.8 per cent).

Based on Ban's small-scale smelting tests (2.5 kg batches) carried out in a DC furnace the following empirical relations were established:

$$\log (\% Ti_2O_3) = 1.781 - (0.025)(\% FeO) \ldots (II)$$

The relationship shown in equation (II) was calculated from a graphical representation of the data from Ban (1988). Ban et. al. (1988) also published data for the re-melting of Sorel and RBM slags. The following correlations were found:

$$\text{Sorel slag: } \log(\%\ Ti_2O_3) = 1.795 - (0.040)(\%\ FeO) \quad \ldots(III)$$

$$\text{RBM slag: } \log(\%\ Ti_2O_3) = 1.960 - (0.050)(\%\ FeO) \quad \ldots(IV)$$

Pistorius and Coetsee (2000) also investigated the relationship between FeO and Ti_2O_3 in ilmenite smelter slags. The following relationships were found for South African (includes slag from Iscor, Namakwa Sands and RBM) and Canadian (QIT) slags respectively:

$$\text{South African slags: } \%\ Ti_2O_3 = (-1.84)(\%\ FeO) + 50.1,\ R^2 = 0.91 \quad \ldots(V)$$

$$\text{Canadian slags: } \%\ Ti_2O_3 = (-1.39)(\%\ FeO) + 34.9,\ R^2 = 0.84 \quad \ldots(VI)$$

Pistorius and Coetsee (2000) found that the FeO-Ti_2O_3 relationship in the ilmenite smelter slags appears to follow a single pattern for different smelter furnace sizes and designs. This relationship is only affected by the impurity content of the feed materials. To quantify the effects of the impurity oxides the following set of equations were used:

$$(\%\ FeO)_{eq} = (\%\ FeO) + (M_{FeO}/M_{MgO})(\%\ MgO) + (M_{FeO}/M_{MnO})(\%\ MnO) \quad \ldots(VII)$$

$$(\%\ Ti_2O_3)_{eq} = (\%\ Ti_2O_3) + (M_{Ti2O3}/M_{V2O5})(\%\ V_2O_5) + (M_{Ti2O3}/M_{Cr2O3})(\%\ Cr_2O_3) + (M_{Ti2O3}/M_{Al2O3})[(\%\ Al_2O_3) - (\%\ SiO_2)/3] \quad \ldots(VIII)$$

M_i is taken as the molar mass of the oxide i, and the amounts of the oxides are in mass percentages. In equation (VIII) the vanadium content of the slag is expressed as V_2O_5 as this is the convention. Pistorius and Coetsee (2000) point out that the vanadium can however be expected to be in the trivalent form. The equation also shows that some of the Al_2O_3 content is not taken into account when the equivalent Ti_2O_3 content is calculated. The reason given for this is that some of the Al_2O_3 reports to a separate glass phase. It should be noted that the partitioning of other oxides (such as MnO and FeO) were not taken into account by Pistorius and Coetsee (2000). After taking into account the effect of the impurity oxides, and normalisation of the data, it was found that the slag compositions closely follows that expected for the stoichiometric M_3O_5 composition, with the end members of the M_3O_5 composition relevant to ilmenite smelting are $FeTi_2O_5$ and Ti_3O_5. The relationship between Ti_2O_3 and FeO according to the stoichiometric M_3O_5 composition can be expressed by equation (IX):

$$\%\ Ti_2O_3 = (-2.07)(\%\ FeO) + 64.28 \quad \ldots(IX)$$

2.2.3 LIQUIDUS AND TAPPING TEMPERATURES APPLICABLE TO ILMENITE SMELTING

The components most relevant to high titania slags are TiO_2, Ti_2O_3 and FeO (see Table 9). Several phase diagrams relevant to these systems have been published. Eriksson and Pelton (1993) critically evaluated the available thermodynamic and phase diagram data for all the phases in the FeO-TiO_2 and Ti_2O_3-TiO_2 systems. Their optimised calculated equilibrium diagrams for these systems are shown in Figure 7 and Figure 8.

Figure 7 : Optimised FeO-TiO_2 phase diagram (Eriksson and Pelton, 1993)

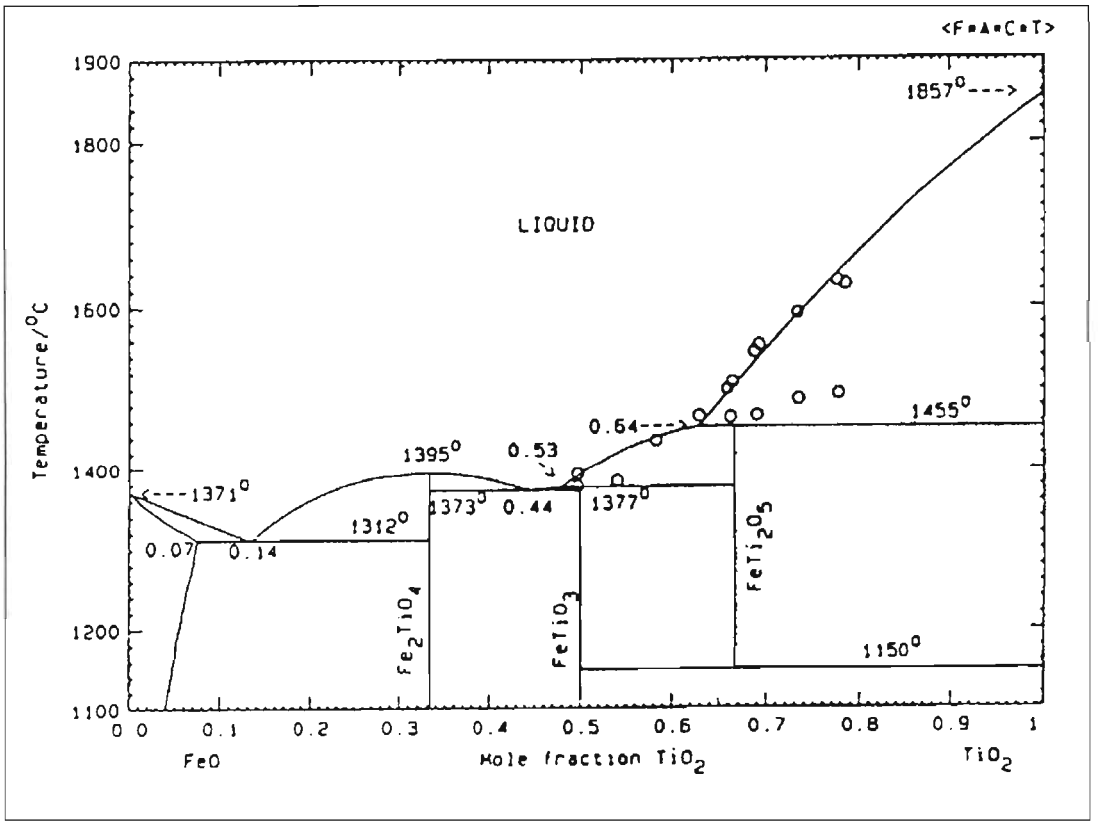

Figure 8 : Optimised Ti_2O_3-TiO_2 phase diagram (Eriksson and Pelton, 1993)

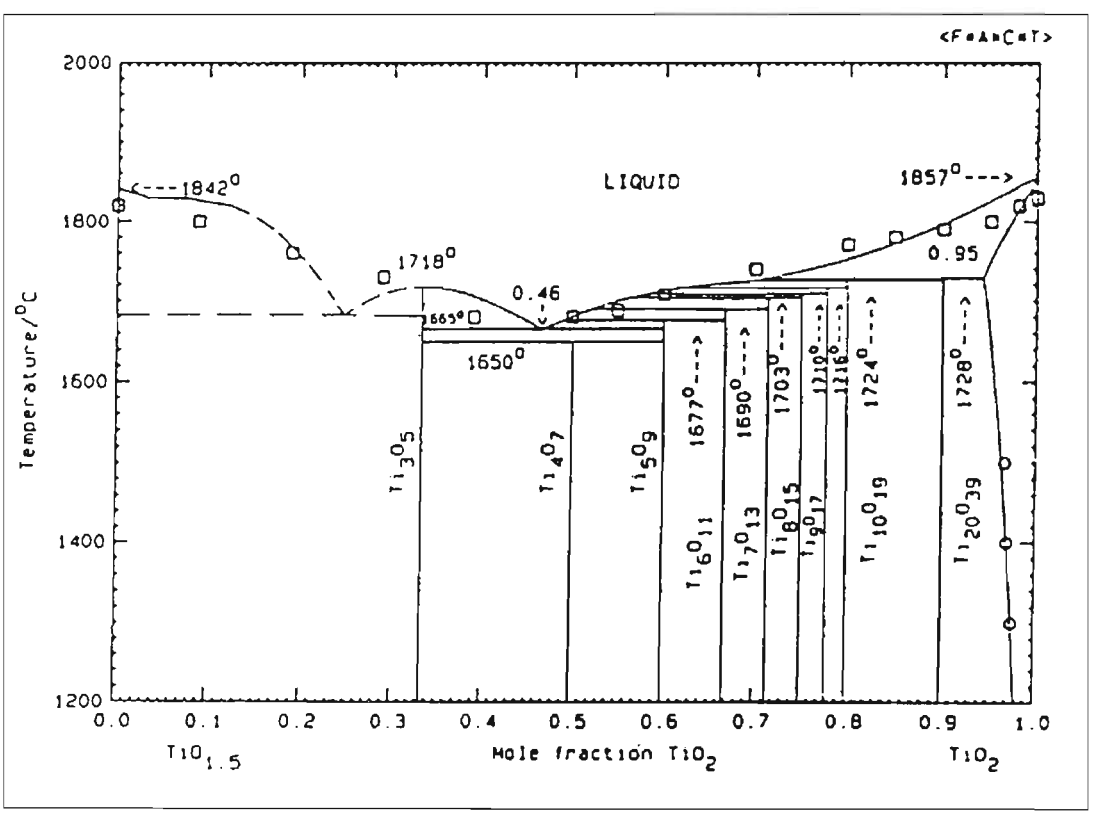

Pesl (1997) carried out isothermal experimental work on the FeO-TiO_2-$TiO_{1.5}$ ternary system at 1500 and 1600 °C. The phase diagrams for these two temperatures are shown in Figure 9 and Figure 10 respectively. Oxygen isobars relevant to the phase diagrams are also shown. The system consists of liquid slag, which has saturation boundaries with metallic iron, rutile, M_3O_5 and M_8O_{15}. For the 1600 °C isotherm it was found that the liquid slag region is enlarged substantially compared to the 1500 °C isotherm. Double saturation with respect to metallic iron and the M_3O_5 phase at 1600 °C was found to occur at 16 mol per cent FeO and 39 mol per cent $TiO_{1.5}$.

Figure 9: FeO-TiO_2-$TiO_{1.5}$ isothermal phase diagram – 1500 °C (from Pesl, 1997)

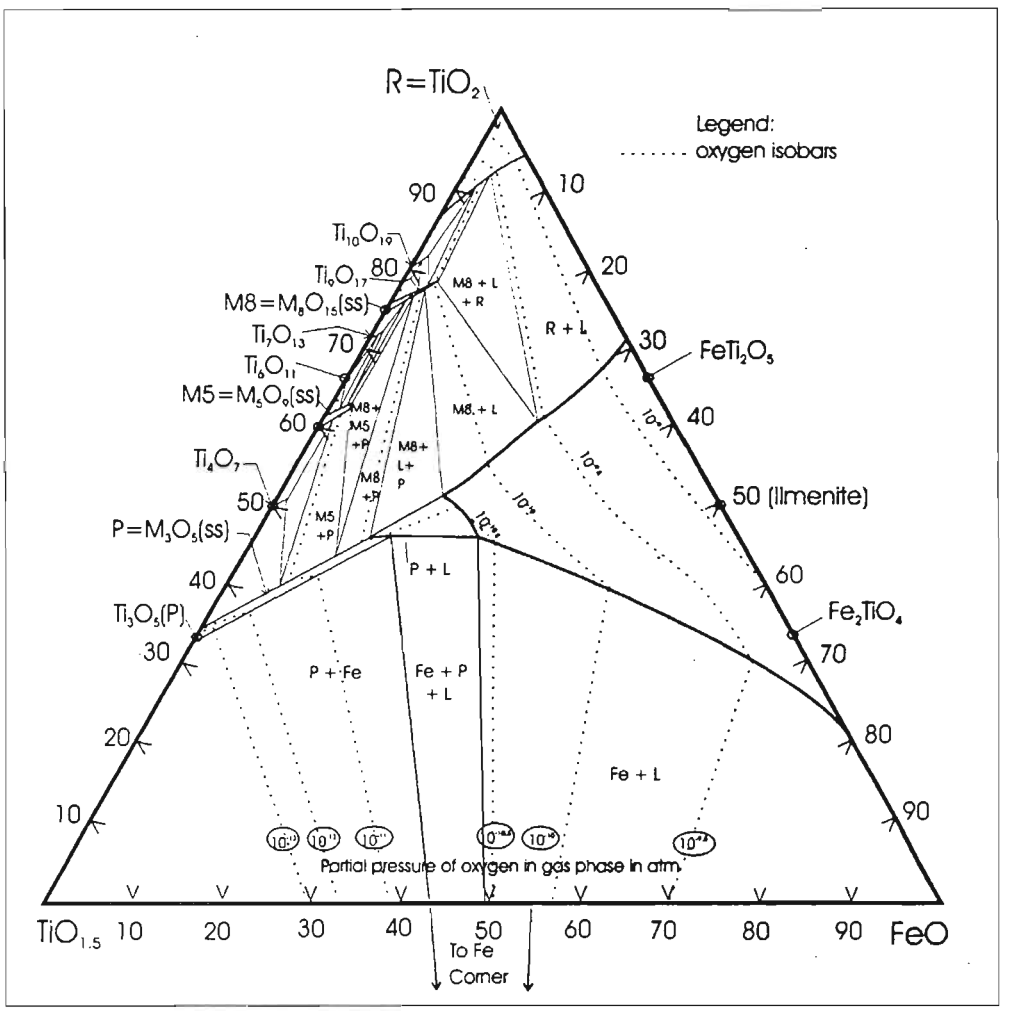

Pistorius and Coetsee (2000) presented a conjectural liquidus diagram of the system $FeTiO_3$-TiO_2-$TiO_{1.5}$, relevant to ilmenite smelter slags (see Figure 11). This diagram was based on the FeO-TiO_2 and Ti_2O_3-TiO_2 binary diagrams of Eriksson and Pelton (1993), as well as data from Pesl (1997). Quasichemical model parameters for the liquid slag region taken from Eriksson and Pelton (1993) were used to calculate the slag composition in equilibrium with iron. Based on this diagram it was proposed that the formation of Ti_2O_3 does have a beneficial effect of lowering the liquidus temperature of the slag.

Grau and Poggi (1978) described the Sorel slag tapping data they obtained from smelting testwork in their 150 kVA pilot furnace. These results are shown in Figure 12 as a function of

the equivalent per cent TiO_2 (total Ti expressed as TiO_2). Also shown in Figure 12 are the melting point data of the Sorel slags.

Figure 10: FeO-TiO_2-$TiO_{1.5}$ isothermal phase diagram – 1600 °C (from Pesl, 1997)

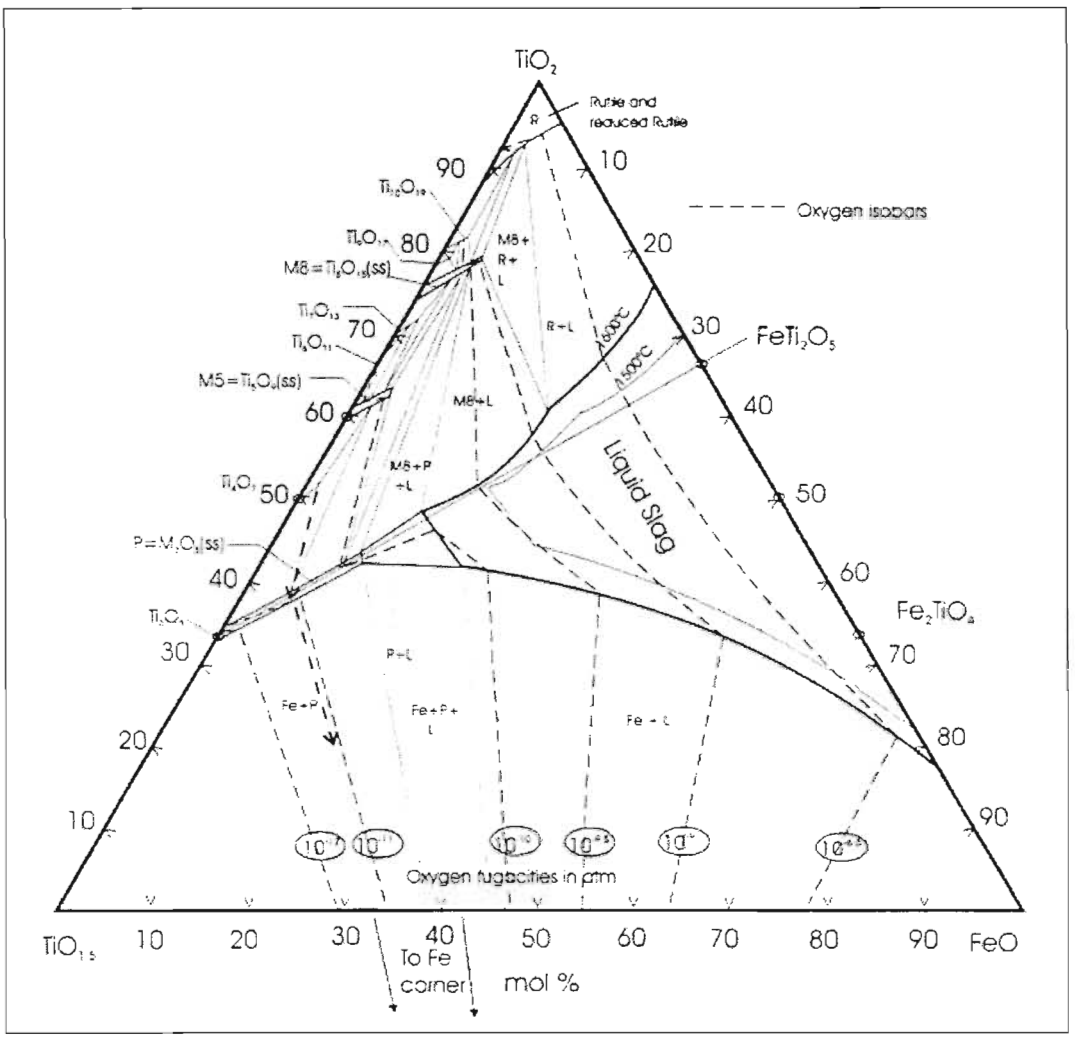

These melting points were determined by the cooling curve technique. With this technique slag temperature is continuously recorded during a cooling cycle, with a temperature arrest during cooling indicating the start of solidification. This was taken as the melting point, or liquidus temperature, of the particular slag. The results show that the slag melting point increases approximately linearly with the equivalent TiO_2 content of the slag. The comparison between the slag tapping temperatures and melting points indicates that the difference between the two becomes less as the degree of reduction of the slag increases. The difference between the two values can also be described as the "degree of superheat" within the slag.

In his work Ban (1988) suggested that by relating the liquidus temperature increase of the slag to the FeO content in high titania slags, the melting temperature follows the liquidus line in the $FeTiO_3$-TiO_2 system given by Grau (1979). Based on this Ban (1988) provided the following equation for the liquidus temperature of the slag:

$$\text{Liquidus temperature} = (-8.02)(\%\ \text{FeO}) + 1780 \quad \ldots(X)$$

Figure 11: Conjectural liquidus diagram of the $FeTiO_3$-TiO_2-$TiO_{1.5}$ ternary system (Pistorius and Coetsee, 2000)

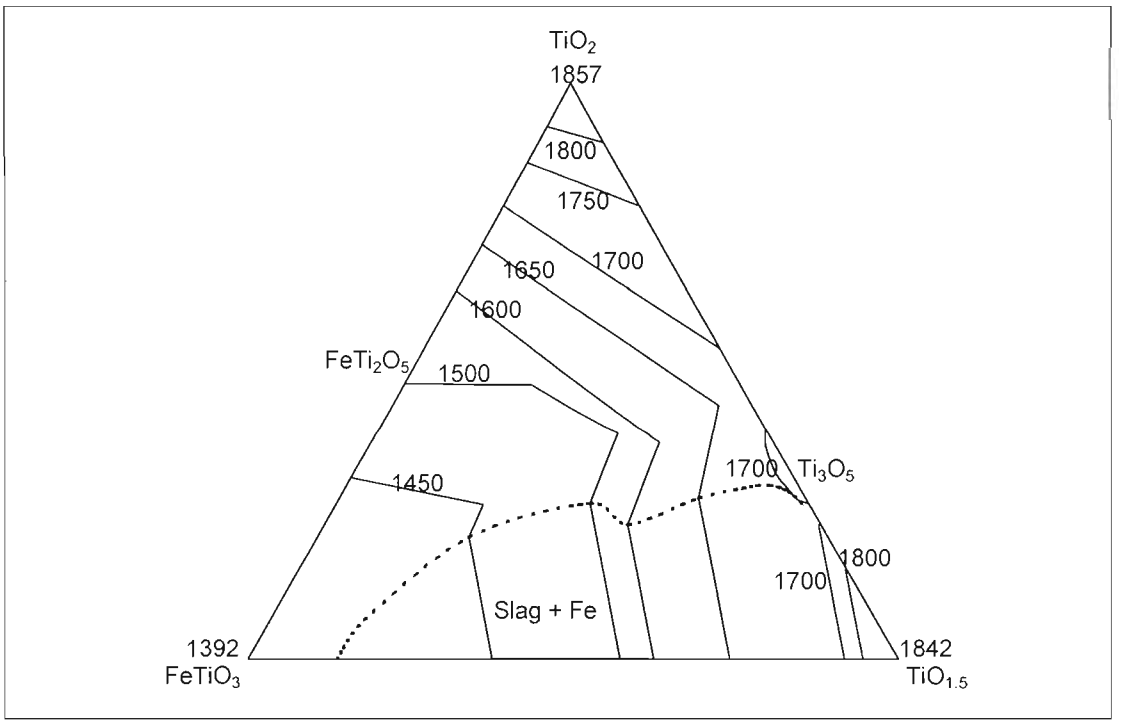

Figure 12: Sorel slag tapping and melting temperatures (Grau and Poggi, 1978)

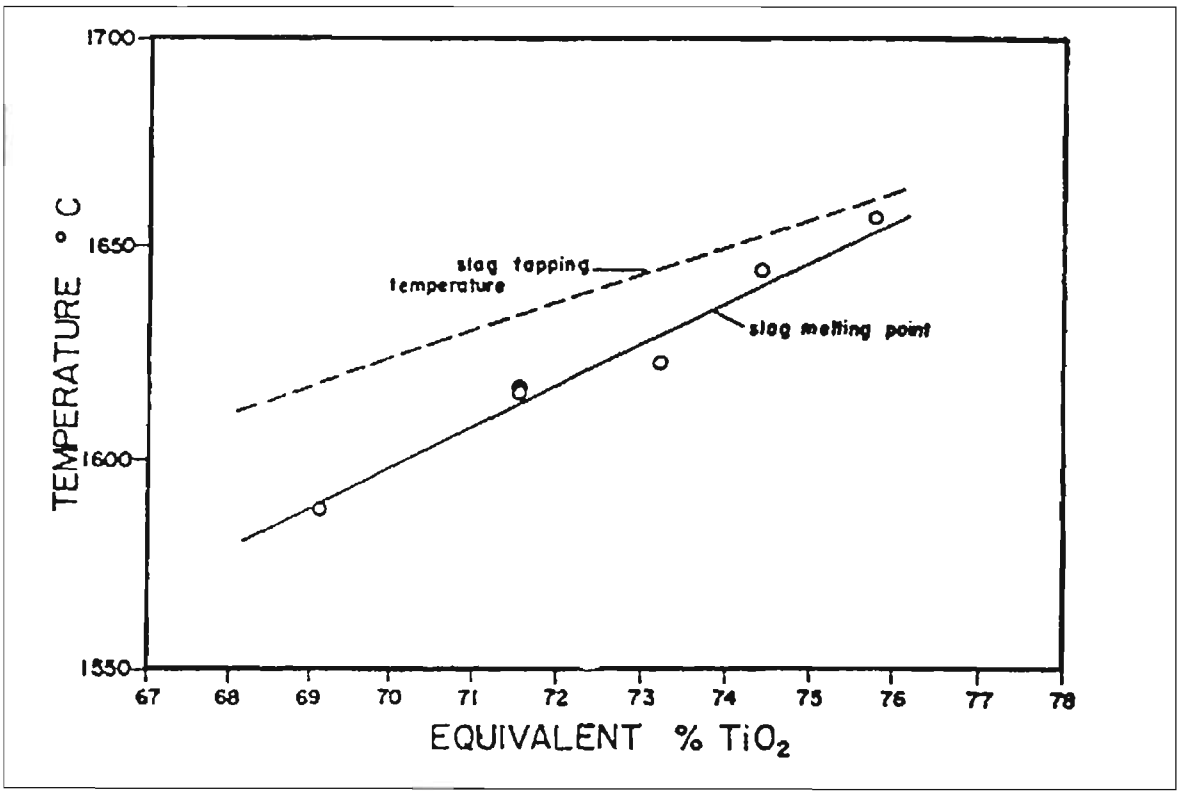

Du Plooy (1997) investigated the melting points of TiO_2-rich slags using a thermal analysis technique. The liquidus temperatures of several industrial slags in various atmospheres were determined as a function of the FeO content of the slags. These results are shown in Figure 13. The total titanium content of the slags (expressed as TiO_2) ranged from 80 to 92 per cent. The oxygen potentials for the various slags were calculated to be approximately the following order of magnitude (the actual values differed somewhat as a function of temperature):

- Ar – Oxygen partial pressure of $10^{-5.9}$ atm.
- CO - Oxygen partial pressure of 10^{-15} atm.
- CO_2 - Oxygen partial pressure of 10^{-2} atm.
- CO/CO_2 - Oxygen partial pressure of 10^{-7} atm.

Figure 13: Liquidus temperatures of various industrial titania slags as a function of the FeO content (Du Plooy, 1997)

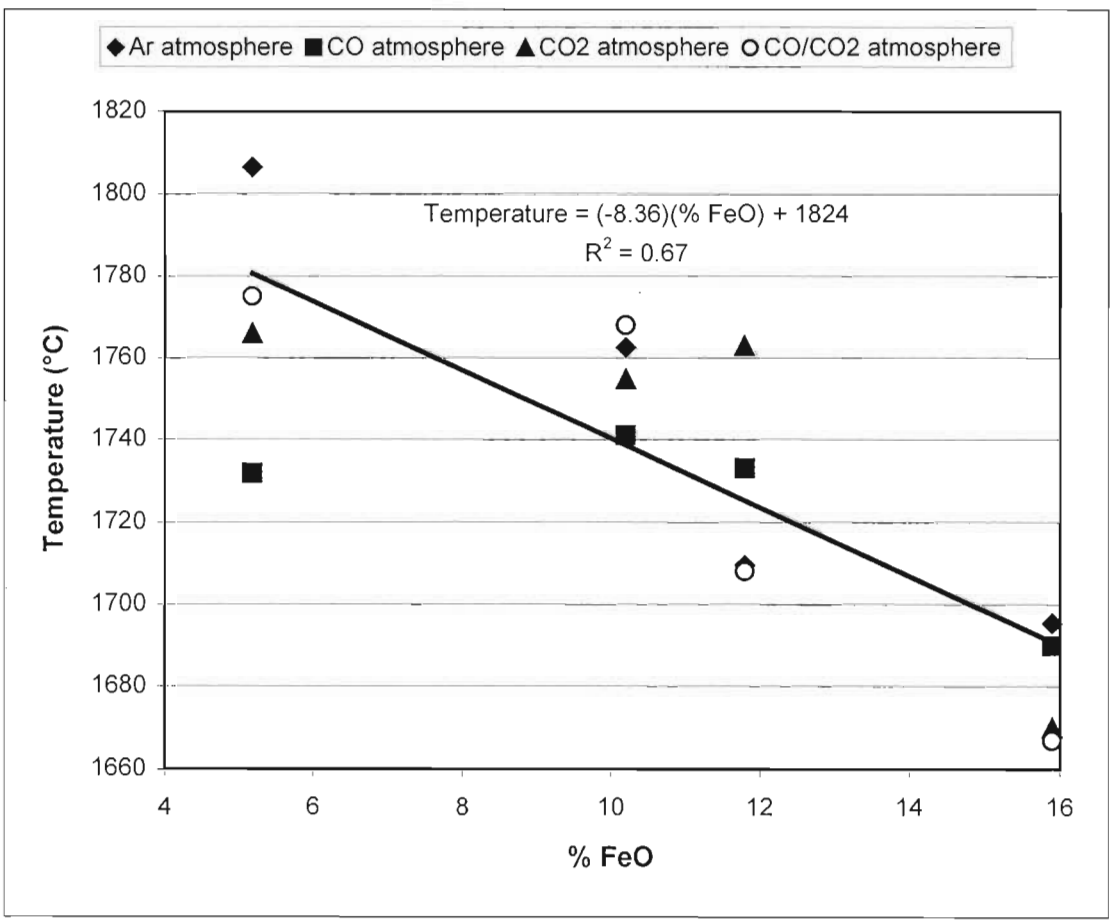

Also shown in Figure 13 is the calculated linear regression line for all the data points.

2.2.4 OTHER ASPECTS OF HIGH TITANIA SLAGS

As the viscosity and electrical characteristics of titania slags are also important in the ilmenite smelting process, a brief review on the available information is given here.

2.2.4.1 Viscosity of titania slags

In the seventies some pioneering work was carried out in determining the viscosity of high titanium slags (Handfield and Charette, 1971; Handfield, Charette and Lee, 1971). They measured the viscosity of Sorel slags (67-80 % TiO_2, 3.3-15 % FeO) using the rotation method. A commercially available viscosity meter (Brookfield Rheolog) was used in the studies. With this method a cylinder is immersed in a crucible containing the slag. The inner cylinder (spindle) is driven by a synchronous motor through a calibrated spring. The deflection of the spring caused by a viscous drag opposing the rotation of the spindle is an indication of the viscosity of the slag. Both the crucible and spindle were made of molybdenum for these studies.

A literature survey conducted by Handfield and Charette (1971) on the viscosity of oxide mixtures containing more than 50 % TiO_2 could not find any papers published prior to 1957. After 1957 the U.S.S.R. Academy of Sciences published a series of articles dealing with the electric melting of titanium slags. Their main conclusions were that the slags investigated had low viscosities when molten. Ti_2O_3, Al_2O_3 and MgO additions increased the viscosity of the slags, with Ti_2O_3 having the largest effect. It was also found that FeO, MnO, CaO and Cr_2O_3 decreased the viscosity of the titanium slags. The composition range over which these results were obtained is not clear from the article.

In their own research Handfield and Charette (1971) used eleven Q I T slags. The composition ranges of the slags were as follows:

TiO_2	67-80 %	Ti_2O_3 as TiO_2	5-26 %
FeO	3.3-15 %	Fe as metal	0.1-1.3 %
SiO_2	3.4-5.4 %	CaO	0.75-0.89 %
MgO	5.2-5.7 %	C	0.02-0.31 %

Figure 14 shows typical results obtained by the researchers. These results show that the viscosity of titania slags is low when completely molten, with values of approximately 30 centipoise.

Smelting of Australian ilmenite was carried out by Swinden and Jones (1978) using an electric arc furnace. The chemical composition of the slags produced was approximately as follows:

TiO_2 (total)	89 %	TiO_2 (actual)	56 %
Ti_2O_3 (actual)	30 %	FeO	10 %
Al_2O_3	1.3 %	MnO	1.5 %

The ternary plot in Figure 15 shows that the slag compositions obtained during the testwork lie on or about the $FeTi_2O_5$-Ti_3O_5 tie line. For the purposes of their study, the small amounts of gangue were grouped together with the FeO content in the slags. It has been found that there is complete miscibility between $FeTi_2O_5$ and Ti_3O_5 above 1346 °C (Grey and Merrit, 1981). This is also shown in Figure 5.

Figure 14 : Viscosity of two typical Sorel slags and of a CaO-TiO_2 mixture (Handfield, Charette and Lee, 1971)

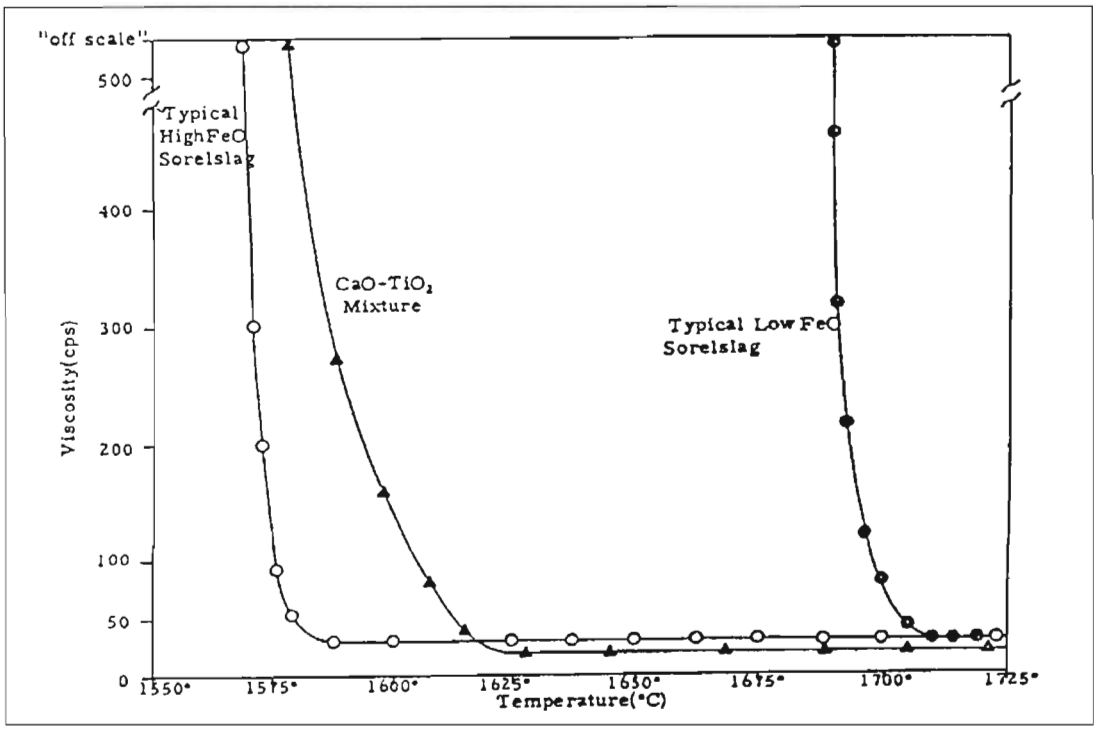

Figure 15 : Slag compositions from the smelting of ilmenite. Fluidity values (mm channel length) adjacent to points (Swinden and Jones, 1978)

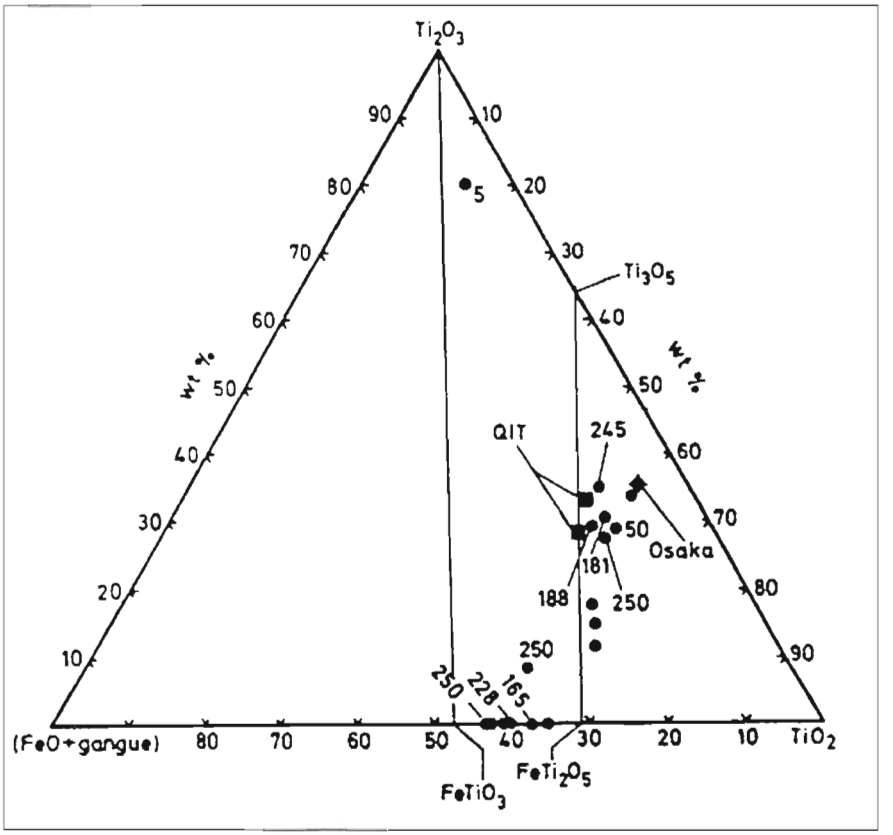

The fluidity of the various slag compositions was determined by pouring the slag into a steel mould with a horizontal tubular channel of 6 mm diameter. The more fluid slags ran further along the channel before solidifying. The fluidity values are therefore expressed as mm channel length. From the few results shown in Figure 15 it seems that in the early stages of the reduction process the melt becomes more viscous as the composition changes from $FeTiO_3$ to $FeTi_2O_5$. As the slag moves along the M_3O_5 solid solution line the slag fluidity seems to increase again. Swinden and Jones (1978) speculated that this could be due to the increasing Ti^{3+} content or to the enrichment of impurities such as MgO and MnO, which act as network breakers in the slag structure. In the Ti_2O_3 corner of Figure 15 the fluidity is extremely low. This suggests that a high slag fluidity might be because of the impurity content and not the Ti^{3+} content.

It is expected that the viscosities of the high titanium slags in this study will be of the same order (30 cps).

2.2.4.2 Electrical conductivity of titania slags

Studies on the electrical conductivity of high titanium slags were carried out by Desrosiers et. al. (1980), using Sorel and RBM slags. Measurements were carried out between 1527 and 1702 °C, with slag compositions ranging between 65 and 90 % TiO_2. Alternating current resistance measurements were made by an impedance bridge at a frequency of 1 kHz. The slag samples were contained in a molybdenum crucible that also acted as a fixed electrode (attached to the bridge by a molybdenum assembly). A molybdenum electrode was placed in the slag to make the necessary measurements. The experimental results obtained by Desrosiers et. al. (1980) are shown in Figure 16.

These results show that the slags are highly conductive, and that the conductivity of the slags increases with increasing TiO_2 content. The RBM slags are significantly more conductive compared to the Sorel slags due to a lower gangue content. In conclusion it was found that the slags were characterized mainly by electronic conduction. The implication of the highly conductive titanium slags is that the best way of operation is in an open-arc mode, with the electrode positioned above the surface of the slag. In such a process the resistive heating of the slag represents a small fraction of the energy delivered to the furnace. Most of the energy is dissipated within the arc and the thermal efficiency of the process relies on the heat transfer from the arc to the molten bath (Grau and Poggi, 1978).

2.3 EXPERIMENTAL DETAILS

2.3.1 SLAG SAMPLES

Various slag samples were obtained during smelting campaigns carried out at the Iscor direct current pilot plant furnace in Pretoria (electrical rating of 1.5 MW). A series of campaigns of varying duration (between 2 to 6 weeks) were carried out between 1995 and 1998. In these campaigns ilmenite was smelted with various carbonaceous reductants to produce high titania slags, with iron metal as a by-product. The titania slag was tapped from the furnace at regular intervals into ladles. The size of each tap ranged from approximately 500 kilogram to approximately one ton. Spoon samples were taken directly from the slag tap stream and

quenched in water, or allowed to cool in air. No differences, chemically and mineralogically, were found between these two types (cooled in water or air) of spoon samples. For the purpose of this study no distinction was made between the two types of spoon samples. These spoon samples were approximately one kilogram in size.

Figure 16 : Variation of electrical conductivity with increasing equivalent TiO_2 content at 1973 K (Desrosiers et. al., 1980)

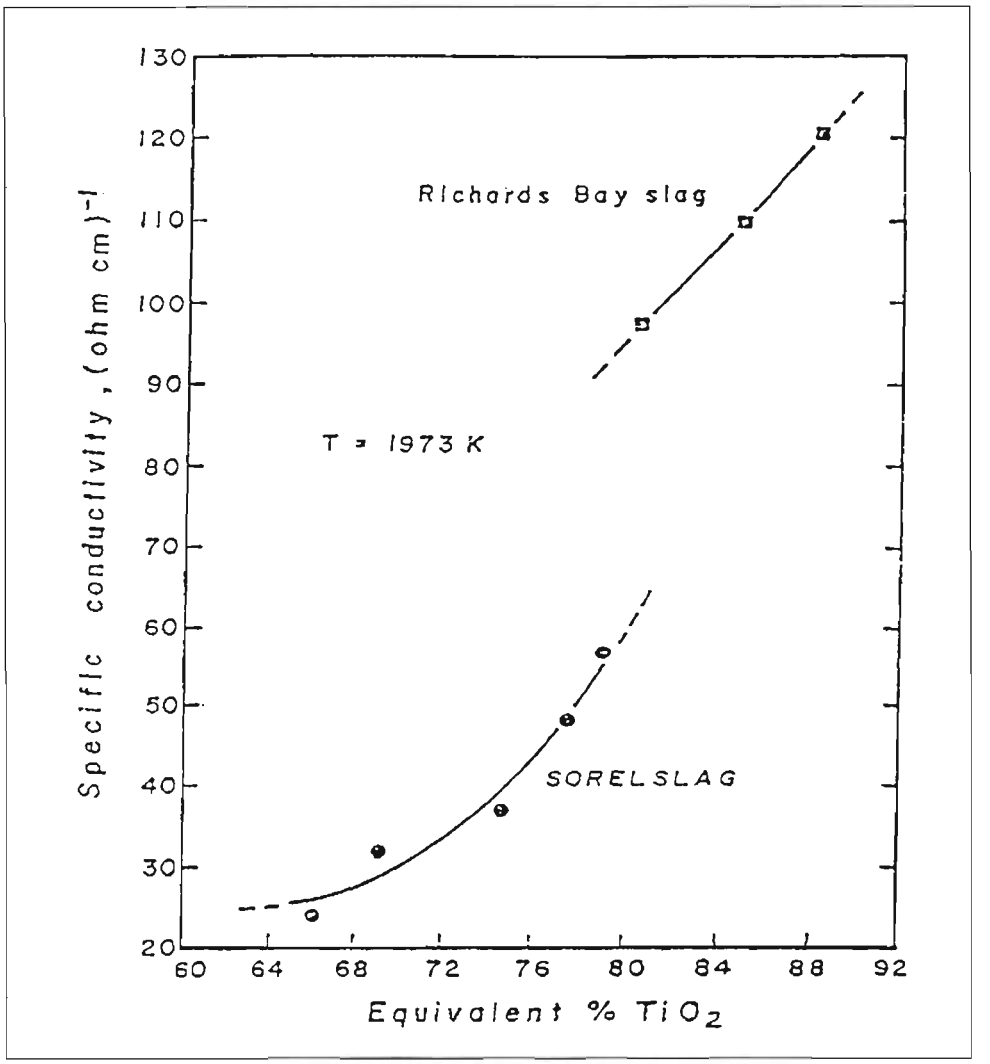

At each slag tap the temperature of the slag was measured with Electronite thermocouple devices (rated to 1730 °C). The temperature of the slag was measured in the ladle, when the ladle was approximately half filled.

2.3.2 ANALYTICAL TECHNIQUES

Chemical analyses of all the samples were carried out using inductively coupled plasma (ICP) or X-ray fluorescence (XRF) instruments. The oxidation states of iron and titanium in the slag samples were determined by using a wet chemical analytical technique (Du Plooy, 1997). X-ray diffraction analyses were also carried out on all the samples. In some instances an internal quartz standard was used to correct the data. In these instances both the M_3O_5 and quartz cell

constants were refined, together with the zero point. The cell constants of quartz were used as a control in these instances. Polished sections were also prepared for standard reflected light microscopy techniques.

2.3.2.1 Scanning electron microscopy and wavelength dispersive analyses

Polished sections of all the relevant samples were made. These polished sections were evaluated by scanning electron microscopy (SEM) and electron microprobe analyses. Photographs of the sample are of back-scattered electron images (unless otherwise indicated), providing contrasts on the basis of atomic numbers.

Suitable areas on the relevant phases were marked on selected polished sections prior to the wavelength dispersive analyses (WDS). An ARL-SEMQ electron microprobe at Mintek was used for the analyses. The elements that were analysed are shown in Table 10. Also shown are the standards that were used for calibration.

Table 10: Standards used for the wavelength dispersive analyses

Element	Standard	Element	Standard	Element	Standard
Mg	Spinel	Zr	ZrO_2 (synthetic)	V	V_2O_5 (synthetic)
Mn	Hausmannite	Al	Spinel	O	Rutile
Ti	Rutile	Fe	Hematite	Cr	Cr_2O_3 (synthetic)
Si	Quartz	Ca	Wollastonite	S	Anhydrite

Rutile was used as standard for oxygen, as most of the samples had both high Ti and O values. For these phases the shifting of the peaks (changing of wavelength of the oxygen X-rays generated and forming of peaks) was not found to be a significant problem. This is an inherent problem with the analyses of the light elements such as carbon and oxygen, where the wavelength of the generated X-rays depends on the bond length between the oxygen atoms and the cations. With this standardisation approach the analysed value for oxygen in the following standards was found to be too low:
Hematite (69.1 per cent Fe): 2.7 per cent too low
Ilmenite (36.2 per cent Fe): 2.1 per cent too low
Quartz (46.7 per cent Si): 5.2 per cent too low.

The error in the analysis of the oxygen content also has implications for the calculation of cation oxidation states. For example, for the calculation of the abundance of Ti^{3+} and Ti^{4+} in a M_3O_5 phase the Ti^{4+}/Ti^{3+} ratio can be greatly understated, depending on the value used for the oxygen analysis. In this study no corrections were applied to the actual observed results for the various phases analysed.

2.3.2.2 Mössbauer spectroscopy

Mössbauer spectroscopy measurements were carried out at the laboratory situated within the Department of Physics at the University of the Witwatersrand. Iron containing samples in powdered form were provided to the laboratory. The ^{57}Fe Mössbauer measurements were carried out in conventional transmission geometry at room temperature. A K3 Austin

Associates linear motor, driven by a triangular reference wave form, were used to scan the resonance profile. A Xe-CO_2 proportional counter was used to detect the transmitted 14.4 keV resonance radiation from a 5-10 mCi $^{57}Co(Rh)$ radioactive source. Typically 40-50 mg.cm^{-2} of sample was used. This was considered the optimal thickness in order to ensure the following:

- Avoid spectral lineshape distortions.
- Ensure acceptable transmission of the incident radiation when taking into account electronic absorption effects.
- Have adequate quantities of the ^{57}Fe isotope in the sample to ensure satisfactory signal-to-noise ratios after typical 12 to 24 hour data accumulation periods.

Data analyses were done by using a non-linear least squares Mössbauer analysing program NORMOS (supplied by WISSEL Starnberg-Germany). The fitting program was used for theoretical fits of the data with Lorentzian lineshapes to deconvolute various sub-components (phases) in the spectrum. A minimum number of sub-spectra (doublets and sextets) was used to obtain the best fit to the total spectrum. Final parameters of the fitted components were compared with the accepted literature values for the various oxides to enable phase identification. Mössbauer interaction parameters of selected Fe-Ti-O compounds relevant to this study are shown in Table 11 (data from Mulaba and Hearne, 1999). These parameters were determined at room temperature. Oxidation states of iron in the various phases were determined from the combination of values of fitted δ (isomeric shift) and Δ (quadrupole splitting) parameters obtained for quadrupole doublets, or from the B_{hf} (internal magnetic field) value of magnetically split sextets.

2.4 RESULTS AND DISCUSSION

2.4.1 MINERALOGICAL ANALYSES OF THE SLAGS

Four main mineralogical phases were identified to be present in the various slags. The amount of the phases varied from slag to slag depending on the chemistry of the slag, as well as the conditions under which each slag was cooled down. Differences were found for example between samples taken from slag blocks (cooled relatively slowly) and spoon samples (cooled relatively quickly).

2.4.1.1 The M_3O_5 phase

The major phase present in the various high titania slags was found to be the M_3O_5 phase. This is illustrated by the micrograph of a typical slag shown in Figure 17, with the M_3O_5 phase indicated by the symbol t. Identification and characterisation of the M_3O_5 phase were done by X-ray diffraction, microprobe analyses and Mössbauer spectroscopy. The bulk compositions of some of these slags characterised by these techniques are shown in Table 12. The phase analyses for these samples were determined from the elemental analyses of the respective phases. The analyses were normalised in order to obtain the number of cations for every five oxygen atoms. The calculated M_3O_5 phase compositions are as follows (full details given in Appendix B):

- DB100 – $Mg_{0.07}Al_{0.04}V_{0.01}Mn_{0.01}Ti_{2.61}Fe_{0.27}O_5$ ($M_{3.01}O_5$)
- DB152 – $Mg_{0.07}Al_{0.09}V_{0.01}Mn_{0.01}Ti_{2.84}Fe_{0.07}O_5$ ($M_{3.09}O_5$)
- DB156 – $Mg_{0.05}Al_{0.08}V_{0.01}Mn_{0.01}Ti_{2.65}Fe_{0.20}O_5$ ($M_{3.00}O_5$)

Table 11: Mössbauer hyperfine interaction parameters of selected Fe-Ti-O compounds at 300 K (Mulaba and Hearne, 1999)

Chemical formula	Mineral name	Ionic state of iron	δ_{Fe} ($mm.s^{-1}$)	Δ ($mm.s^{-1}$)	B_{hf} (T)	Comments	References
Fe	Iron	0	0	0	33.0	bcc metal	-
$FeTiO_3$	Ilmenite	3+	0.27	0.29	-	-	Stevens et. al. (1998)
		2+	1.04	0.70	-		
Fe_2O_3	Hematite	3+	0.37	-0.20	51.1	-	Stevens et. al. (1998)
Fe_2TiO_4	Ulvöspinel	2+	1.16	1.52	-	Inverse spinel where Fe^{2+} is found in "A" site and $Fe^{2+}Ti^{4+}$ in "B" site	Stevens et. al. (1998)
Fe_3O_4	Magnetite	3+ (A)	0.28	0.0	48.7	Tetrahedral – "A" site	Stevens et. al. (1998)
		3+ (B1)	0.66	0.08	45.4	Octahedral – "B" site	
		2+ (B2)	0.63	-0.16	45.7	Octahedral – "B" site	
Fe_2TiO_5	Pseudobrookite (ferric)	3+	0.39	0.70	-	-	Shirane et. al. (1962)
		3+	0.38	0.90	-	When some Fe^{3+} replaces Ti^{4+}, these hyperfine parameters may be obtained	Stevens et. al. (1998)
		3+	0.38	0.56	-		
$FeTi_2O_5$ (with Mg as impurity)	Pseudobrookite (ferrous)	2+	1.05	3.15	-	Tetrahedral - "A" site	Stevens et. al. (1998)
		2+	1.02	1.96	-	Octahedral – "B" site (less intense)	
$FeTi_2O_5$ (with Mn as impurity)	Pseudobrookite (ferrous)	2+	1.05	3.20	-	Tetrahedral - "A" site	Stevens et. al. (1998)
		2+	1.02	2.18	-	Octahedral – "B" site (less intense)	
$FeTi_2O_5$ (with Mn as impurity)	Pseudobrookite (ferrous)	2+	1.17	2.83	-	Tetrahedral - "A" site	Teller et. al. (pp. 351-367, 1990)
$Fe_{0.5}Mg_{0.5}Ti_2O_5$	Armalcolite	2+	1.05	3.15	-	Tetrahedral - "A" site	Stevens et. al. (1998)
		2+	1.03	2.01	-	Octahedral – "B" site (less intense)	
$Fe_2Ti_3O_9$	Pseudorutile	3+	-	-	-	No parameters have been reported	-

δ_{Fe} – Isomeric shift

Δ - Quadrupole splitting

Figure 17: Micrograph of a typical high titania slag

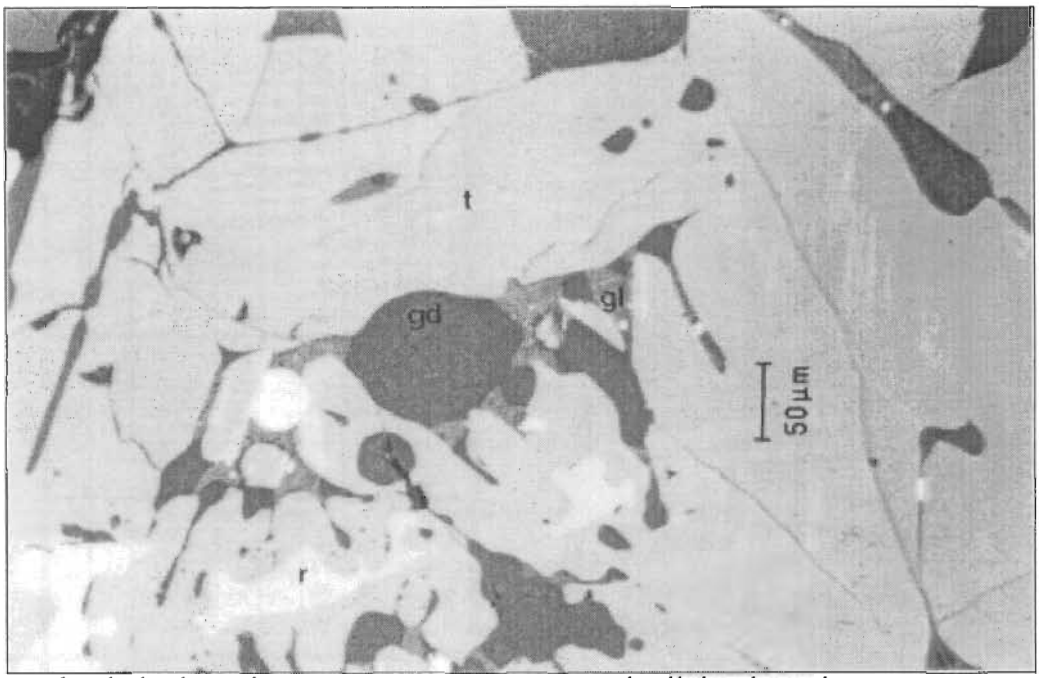

gd – dark glass phase
gl – light glass phase
t – M_3O_5 phase
r – rutile phase

Small amounts of zirconium and chromium were also analysed to be present, but in such small amounts to be ignored for the purposes of this study. The M_3O_5 phases were also analysed for silicon, calcium and sulphur, but only trace amounts of these elements were only found on occasion. It is interesting that the most reduced of these slags, sample DB152 (FeO content of 6.8 per cent and Ti_2O_3 content of 36.8 per cent), has a slight deviation from the M_3O_5 stoichiometry. For this sample a value for M of 3.09 was calculated. A standard deviation value of 0.06 was calculated for M. There however seems to be a mass balance problem when comparing the bulk analysis of the sample (Table 12) with the M_3O_5 phase analysis given in Appendix B. The bulk FeO content of slag DB152 is 6.8 per cent, but the M_3O_5 phase only contains 1.64 per cent Fe (or 2.1 per cent FeO). It therefore seems that the grain that was analysed is not representative of the bulk sample, perhaps even being a Magnéli phase.

It is interesting to note that Borowiec and Rosenqvist (1985) also found an oxygen deficiency in some of their M_3O_5 solid solution phases. This was in their studies of the phase relations in the Fe-Ti-Mg-O system at temperatures below 1100 °C. The oxygen deficiency was found in solid solutions with a $Ti_3O_5/FeTi_2O_5$ molar ratio of approximately greater than 2. They did not suggest any explanation for this.

The Mössbauer data obtained for these slags are shown in Table 13. The Mössbauer spectra of these samples are given in Appendix C, together with the Mössbauer spectra of all the samples in this study. The Mössbauer data show that the majority of the iron content of the slags is present in the A site of the M_3O_5 structure. This confirms the results

Table 12: Bulk chemical analyses of selected slag samples

Sample no.	Analyses (mass %)											
	SiO_2	Al_2O_3	CaO	MgO	MnO	Cr_2O_3	V_2O_5	Fe^0	FeO	TiO_2	Ti_2O_3	Total Ti as TiO_2
DB100	1.41	1.19	0.27	1.03	1.17	0.05	0.45	< 0.1	9.80	53.9	30.4	87.70
DB152	1.76	1.64	0.24	1.02	1.40	0.09	0.42	0.39	6.83	48.4	36.78	89.29
DB156	1.84	1.48	0.27	1.07	1.33	0.09	0.43	0.19	9.42	52.0	30.92	86.40

Table 13: Mössbauer analyses of selected slag samples

Sample number	Sample origin	Hyperfine interaction parameters			Abundance (atom %)	Attribution
		A ($mm.s^{-1}$)	B ($mm.s^{-1}$)	B_{hf} (T)		
DB100	Sample from tap stream	1.16 (2)	3.35 (4)	-	90 (2)	Fe^{2+} compound (ferropseudobrookite; site A)
		1.09 (2)	1.83 (4)	-	10 (2)	Fe^{2+} compound (ferropseudobrookite; site B)
DB152	Sample from tap stream	1.07 (3)	3.00 (5)	-	75 (5)	Fe^{2+} compound (ferropseudobrookite; site A)
		1.07 (2)	1.85 (3)	-	25 (4)	Fe^{2+} compound (ferropseudobrookite; site B)
DB156	Sample from tap stream	1.08 (2)	3.03 (3)	-	82 (5)	Fe^{2+} compound (ferropseudobrookite; site A)
		1.04 (3)	2.0 (5)	-	15 (5)	Fe^{2+} compound (ferropseudobrookite; site B)
		0.49 (3)	0.68 (2)	-	3 (3)	Fe^{3+} compound (pseudobrookite)

Errors are quoted in brackets

obtained by other investigators (see data shown in Table 4 and Table 5). It is also interesting to note that the most reduced slag (DB152, composition closest to Ti_3O_5) has the lowest iron content in the A site. This confirms the findings of Grey and Ward that the iron content in the A site decreases with a decrease in the iron content of the M_3O_5 phase. The data in Table 13 also show that the oxidation state of the iron contained in the high titania slags are +2. For sample DB156 the presence of some Fe^{3+} was indicated. This was however discounted due to the large relative error of the result, with the error being equal to the value.

X-ray diffraction data obtained for the M_3O_5 phase in a typical slag (sample DB156) are shown in Table 14. Only the major peaks are shown, with the detailed set of data given in Appendix D. Also given in Appendix D is the calculated data for the phase. As discussed previously (see Table 6) the two major peaks (at approximately d = 3.50 Å and d = 2.76 Å) for the M_3O_5 phase were also found in this sample. X-ray diffraction patterns for the slag samples given in Table 12 are shown in Appendix E. These patterns also include the pattern for quartz that was used as internal standard.

Table 14: Crystallographic data for sample DB156

h	k	l	d (Å)	I/I_0 (obs)
2	0	0	4.910	36.0
2	0	0	4.898	16.9
1	1	0	3.531	100.0
1	1	0	3.522	51.5
2	0	3	2.760	79.2
2	0	3	2.753	39.1
3	1	0	2.473	20.9
1	1	3	2.425	20.8
2	0	4	2.230	15.1
4	0	2	2.201	18.8
4	0	3	1.975	21.0
0	2	0	1.890	35.1
0	2	0	1.886	18.1
5	1	2	1.644	20.0
2	2	3	1.559	21.0
5	1	3	1.543	18.0

The unit cell parameters obtained for the M_3O_5 phases in the titania slag samples are shown in Table 15. The data shows that low standard deviations were obtained for all the samples. The difference in volume between the highest (DB100) and lowest (DB152) cell volume is approximately 0.2 per cent.

The site occupancies of the cations in the M_3O_5 structure were calculated by using all the available information, together with some assumptions. The results of the calculations are shown in Table 16. The information used, and the assumptions made, are listed below:

- The elemental phase analyses data for the various samples given in Appendix B were used to determine the composition of the M_3O_5 phase in each sample, as well as for the

calculation of the charge balance. To calculate the charge balance the following were taken into consideration:

- Iron is only present in the +2 oxidation state (based on Mössbauer results – see Table 13).
- Magnesium and manganese are only present in the +2 oxidation state, aluminium in the +3 oxidation state.
- Vanadium is present in the +3 oxidation state (see Pistorius and Coetsee, 2000).
- The Ti^{3+} and Ti^{4+} contents were calculated using the composition data. This was done by assuming a charge balance (the oxidation state of oxygen is –2).

- All the V^{3+} and Al^{3+} report to the smaller B site because of their small cation size ($r(Ti^{3+}) > r(V^{3+}) > r(Al^{3+})$), the larger Mn^{2+} cation reports exclusively to the larger A site (see ionic radii, Table 2).
- Fe^{2+} is distributed among the A and B sites according to the Mössbauer results shown in Table 13.
- One third of the Mg^{2+} is present in the B site. This assumption is made on the basis of the data in Table 5 for $Ti_{2.36}Fe_{0.33}Mg_{0.31}O_5$. It is believed that this information for Mg^{2+} is closest to the slags investigated in this study.
- Ti^{4+} preferentially fills the smaller B site (see Table 4 for distribution of Ti^{3+} and Ti^{4+} in Ti_3O_5).
- Ti^{3+} is distributed according to the remaining available spaces.

Table 15: Unit cell data for the M_3O_5 phases in the respective titania slag samples

Lattice parameters	Sample numbers			
	DB100	DB123	DB152	DB156
a (Å)	9.7830 (0.0003)	9.7770 (0.0007)	9.7939 (0.0003)	9.7915 (0.0024)
b (Å)	3.7794 (0.0001)	3.7599 (0.0002)	3.7769 (0.0001)	3.7768 (0.0007)
c (Å)	10.0122 (0.0004)	10.0649 (0.0007)	9.9902 (0.0003)	10.0010 (0.0027)
Cell Volume ($Å^3$)	370.191 (0.026)	369.988 (0.051)	369.542 (0.014)	369.841 (0.113)

Standard deviation values given in brackets

For samples DB100 and DB152 the stoichiometry was calculated to be $M_{3.01}O_5$ and $M_{3.09}O_5$ respectively (see Appendix B). In Table 16 the additional cations were included in the B site for calculation purposes. For example the stoichiometry for DB152 was calculated to be $A_{1.00}B_{2.09}O_5$.

The Ti^{3+} fraction (as a fraction of the total Ti in moles) of the M_3O_5 phase was found to be approximately 0.5 for samples DB100 and DB156 (see Table 16). This might however be too high due to the error associated with the oxygen analysis. Based on the bulk chemical analyses of these samples this value is closer to 0.4 (see Table 12).

2.4.1.2 Rutile phase

Rutile was identified as the second most prevalent phase in the slags as identified by X-ray diffraction. Figure 17 also shows the presence of the rutile phase (r). Microprobe analysis of a typical rutile phase is given in Table 17, showing that the phase consists mainly of titanium as expected. It was however not possible to determine whether all the titanium is in the +4 oxidation state, or whether there is some Ti^{3+} present. This is because the oxygen content of the phase was not determined. The analysis also shows some solubility of manganese and iron in the rutile. Webster and Bright (1961) however found limited solubility of iron in rutile at 1200 °C.

Table 16: Proposed cation distribution in the M_3O_5 phases present in titania slags

Sample no.	A site	B site
DB100	$Fe^{2+}_{0.24}\ Mn^{2+}_{0.01}\ Mg^{2+}_{0.05}\ Ti^{3+}_{0.70}$	$Fe^{2+}_{0.03}\ Mg^{2+}_{0.02}\ Al^{3+}_{0.04}\ V^{3+}_{0.01}\ Ti^{3+}_{0.59}\ Ti^{4+}_{1.32}$
DB152	$Fe^{2+}_{0.05}\ Mn^{2+}_{0.01}\ Mg^{2+}_{0.05}\ Ti^{3+}_{0.89}$	$Fe^{2+}_{0.02}\ Mg^{2+}_{0.02}\ Al^{3+}_{0.09}\ V^{3+}_{0.01}\ Ti^{3+}_{1.07}\ Ti^{4+}_{0.88}$
DB156	$Fe^{2+}_{0.17}\ Mn^{2+}_{0.01}\ Mg^{2+}_{0.03}\ Ti^{3+}_{0.79}$	$Fe^{2+}_{0.03}\ Mg^{2+}_{0.02}\ Al^{3+}_{0.08}\ V^{3+}_{0.01}\ Ti^{3+}_{0.60}\ Ti^{4+}_{1.26}$

Table 17: Microprobe analysis of a typical rutile phase (mass percentages)

Total Ti as TiO_2	MnO	FeO
98.08	0.19	1.72

2.4.1.3 Glass phases

Examples of the glass phases found in titania slags are shown in Figure 17. Two types of glass phases were identified, a light coloured phase (identified by gl) and a dark coloured phase (identified by gd). These two phases were found in close proximity to each other. The bulk chemical analysis of the sample shown in Figure 17 is given in Table 18. In terms of the FeO content of the slag it could be characterised as a typical slag that would be produced for the chloride production route. The impurity content, in particular the CaO and SiO_2 content, is however too high.

A summary of the microprobe analyses of the two glass phases identified is given in Table 19 (details given in Appendix F). From Table 19 it can be seen that the dark coloured glass phase consists mainly of SiO_2 and TiO_2. The composition of the light coloured phase is more complex. The main component is once again SiO_2, with TiO_2, MnO, FeO and CaO all present at levels of approximately 10 to 15 per cent. The composition of this glass phase also appears to be similar to that of the Tyssedal slag (see Table 3).

Table 18: Bulk chemical analysis of sample YS2872

Sample no.	Analyses (mass %)											
	SiO_2	Al_2O_3	CaO	MgO	MnO	Cr_2O_3	V_2O_5	Fe^0	FeO	TiO_2	Ti_2O_3	Total Ti as TiO_2
YS2872	2.56	1.60	0.72	0.55	1.18	0.10	0.42	0.03	9.98	49.1	33.5	86.3

Table 19: SEM analyses of the dark and light coloured glassy samples found in sample YS2872

	Analysis (mass per cent)								
	MgO	Al_2O_3	TiO_2	MnO	FeO	SiO_2	K_2O	CaO	Na_2O
Dark coloured phase	-	3.13	8.21	0.61	1.74	83.61	1.10	1.07	0.78
Light coloured phase	-	5.85	11.48	10.76	11.19	45.82	0.13	14.80	-

2.4.1.4 Metallic iron phases

Two types of metallic Fe particles were identified in the Iscor slags. The most prominent particles were finely disseminated metallic iron globules present in the slag and on the grain boundaries of the Ti-oxide crystals, in the silicate rich glassy matrix. The size of these particles was greater than approximately 15 μm, and as large as 150 μm as determined by SEM analyses (apparent diameter as determined in polished section). These metallic globules are believed to consist of metallic iron droplets caught in the slag. Some of these metallic iron globules contained a Fe-sulphide rich outer margin. Microprobe analyses of this Fe-sulphide phase is shown in Table 20, with the Fe:S molar ratio being 0.68. The Fe-sulphide outer rim also contains small amounts of Mn and Ti. The sulphur found in the slags was always associated with the iron globules. Examples of this are shown in Figure 18. The phenomenon of metallic iron globules containing a Fe-sulphide rich outer margin had previously also been observed by Reznichenko et. al. (1981) and Toromanoff and Habashi (1984).

Table 20: Microprobe analyses of the iron sulphide phase on the rim of an iron globule

Element	Analyses (mass %)
S	44.0
Fe	52.1
Mn	2.2
Ti	1.81

The second type of metallic iron particle present in the slags was found to be present in the rutile phases. It was found that the larger of the rutile crystals contained fine, metallic iron precipitates. The size of these precipitates was less than approximately 3 μm. An example of this is shown in Figure 19. Toromanoff and Habashi (1984) found similar precipitates nucleated during cooling of their slags as a result of the following reaction:

$$2\ Ti^{3+} + Fe^{2+} \rightarrow 2\ Ti^{4+} + Fe^{0} \ldots (J)$$

2.4.2 CHEMICAL ANALYSES OF THE SLAGS

The chemical composition of high titania slags is dependent on the chemical quality of the ilmenite and reductant used for smelting. The extent of reduction during the smelting process obviously also has an effect on the chemical composition of the slags, especially so for the iron and titanium content of the slags. In Table 21 a wide range of slag compositions is given. These slags were prepared in the Iscor pilot plant furnace during various ilmenite smelting campaigns. In these campaigns a variety of ilmenite and reductant feedstocks were used, resulting in the range of chemical compositions shown. Also shown in Table 21 is the insoluble content of some selected slags. This analysis refers specifically to the suitability of a particular slag for the sulphate pigment production process, with a high value indicating that the slag is less suitable for the sulphate process. The rutile content of the slag is important in this regard, as rutile is insoluble in sulphuric acid (Stanaway, 1994). As the rutile content of the slags was not quantified, it was not possible to correlate the data in Table 21 with the rutile content.

Figure 18: Micrograph of metallic iron globules (F) with a Fe-sulphide rich outer margin (S)

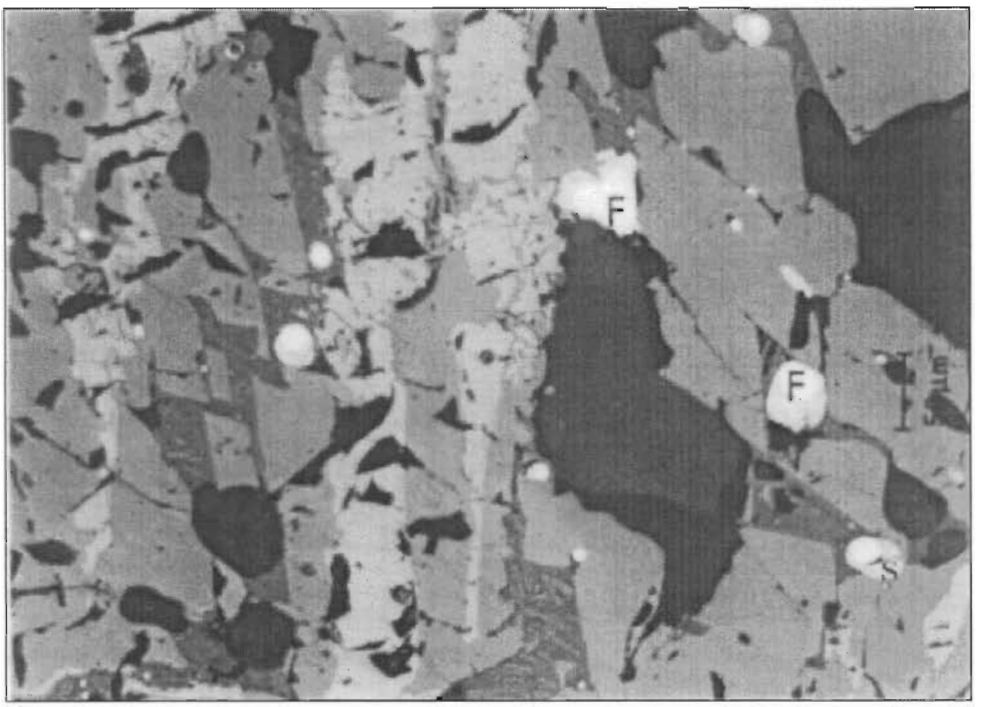

Figure 19: Micrograph of fine metallic iron precipitates (F) within the rutile phase (R)

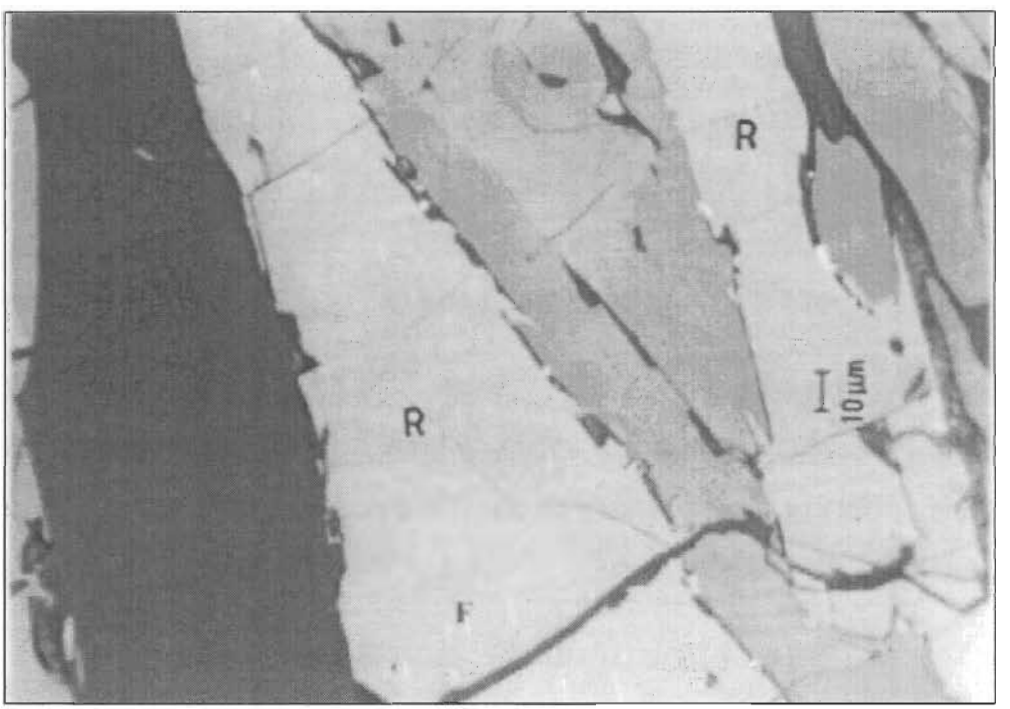

Table 21 : Chemical analyses of various high titania slags produced in the Iscor 3 MVA plasma furnace

Sample no.	Tap Temperature (°C)	Analyses (mass %)															TiO_2 insolubility
		SiO_2	Al_2O_3	CaO	MgO	MnO	Cr_2O_3	V_2O_5	ZrO_2	C	S	Fe^0	FeO	TiO_2	Ti_2O_3	Total Ti as TiO_2	
3176	1641	1.26	0.98	0.10	0.94	1.25	0.13	0.47	-	0.05	0.06	0.06	11.80	55.00	27.90	86.00	-
3179	1662	1.23	1.07	0.12	0.97	1.22	0.12	0.46	-	0.04	0.07	0.17	10.20	51.80	33.20	88.69	-
3191	1669	2.30	1.24	0.25	1.61	1.24	0.09	0.39	-	0.14	0.08	0.13	9.27	54.00	31.00	88.45	-
3206	1735	2.28	1.62	0.47	0.80	1.15	0.10	0.43	-	0.06	0.09	0.06	5.38	45.15	42.20	92.05	3.46
3209	-	2.75	1.59	0.57	0.53	1.24	0.09	0.40	-	0.04	0.04	0.04	10.64	49.50	32.15	85.23	5.17
3215	-	2.10	1.47	0.35	0.93	1.06	0.08	0.43	-	0.02	0.03	0.07	15.65	55.40	22.30	80.18	4.28
3216	1660	1.75	1.11	0.18	0.37	0.86	0.03	0.44	-	0.04	0.05	0.16	13.30	53.00	29.30	85.56	-
3222	1721	1.56	1.04	0.22	1.05	1.03	0.08	0.45	-	-	-	0.20	5.93	47.70	41.70	94.04	-
3228	1706	1.46	1.14	0.39	1.20	1.24	0.11	0.49	-	0.04	0.07	0.06	7.59	39.05	47.00	91.28	5.79
3229	1695	1.48	1.11	0.38	1.20	1.23	0.13	0.51	-	0.05	0.07	0.17	8.58	37.30	47.55	90.14	1.15
4008	1679	1.04	0.58	0.21	1.00	1.23	0.03	0.46	0.35	-	0.06	0.14	11.40	53.60	28.70	85.50	4.05
4009	1668	1.03	0.58	0.22	0.99	1.24	0.03	0.44	0.36	-	0.06	0.09	10.58	56.20	27.50	86.80	5.41
4011	1679	1.03	0.64	0.22	1.52	1.18	0.03	0.47	0.36	-	0.07	0.13	10.19	54.40	29.00	86.60	3.26
4014	1667	1.18	0.66	0.24	1.08	1.22	0.04	0.47	0.36	-	0.09	0.10	11.23	54.50	27.80	85.39	4.57
4016	1676	1.18	0.69	0.21	1.37	1.15	0.03	0.49	0.34	-	0.06	0.09	11.05	56.00	26.90	85.90	-
4022	1678	1.34	0.70	0.24	1.16	1.20	0.03	0.46	0.35	-	0.07	0.09	10.50	56.50	26.70	86.20	3.26
4027	1686	1.26	0.76	0.29	0.99	1.19	0.03	0.47	0.35	-	0.06	0.09	9.64	54.70	28.80	86.70	3.07
4033	1700	0.96	0.69	0.19	1.88	1.05	0.02	0.48	0.34	-	0.06	0.16	8.56	60.60	25.50	88.94	2.90
4040	1679	1.00	0.56	0.19	2.86	1.13	0.03	0.47	0.34	-	0.06	0.27	9.79	55.70	27.30	86.04	1.28
4044	1688	1.32	1.02	0.58	1.99	1.12	0.02	0.47	0.36	-	0.06	0.08	11.31	57.50	24.90	85.17	2.71
6005	1652	1.16	0.71	0.21	2.06	1.20	0.04	0.43	-	-	-	0.23	13.70	55.30	23.30	81.25	-
6006	1639	1.11	0.69	0.19	1.63	1.21	0.04	0.41	-	-	-	0.18	16.10	57.30	19.90	79.47	-
6009	1616	1.09	0.67	0.25	1.40	1.18	0.04	0.41	-	-	-	0.24	17.90	57.90	17.80	77.69	-
6010	1623	1.10	0.67	0.24	1.33	1.17	0.04	0.41	-	-	-	0.23	17.30	58.10	18.20	78.34	-
6012	1648	1.08	0.68	0.20	1.14	1.21	0.04	0.42	-	-	-	0.19	15.70	56.80	21.60	80.81	-

Table 21 : Chemical analyses of various high titania slags produced in the Iscor 3 MVA plasma furnace (Continued)

Sample no.	Tap Temperature (°C)	Analyses (mass %)															TiO_2 insolubility
		SiO_2	Al_2O_3	CaO	MgO	MnO	Cr_2O_3	V_2O_5	ZrO_2	C	S	Fe^0	FeO	TiO_2	Ti_2O_3	Total Ti as TiO_2	
6013	1639	1.17	0.68	0.20	1.16	1.22	0.04	0.42	-	-	-	0.23	14.70	56.10	22.60	81.19	-
6015	1635	1.17	0.67	0.20	1.11	1.27	0.03	0.42	-	-	-	0.32	14.60	57.30	21.90	81.69	-
6021	1688	1.21	0.76	0.23	1.68	1.25	0.03	0.41	-	-	-	0.06	10.50	54.30	28.40	85.81	-
6025	1665	1.63	1.03	0.32	2.62	1.58	0.21	0.40	-	-	-	0.06	10.90	55.40	24.80	81.04	-
6031	1698	1.36	0.81	0.33	1.99	1.30	0.05	0.39	-	-	-	0.03	7.50	49.80	35.40	89.16	-
6033	1707	1.29	0.82	0.29	1.44	1.22	0.04	0.42	-	-	-	0.06	8.80	53.80	31.70	89.04	-
6034	1712	1.26	0.78	0.28	1.31	1.23	0.03	0.42	-	-	-	0.01	8.10	52.90	33.40	89.99	-
6047	1650	2.82	1.17	0.56	1.15	1.37	0.03	0.36	-	-	-	0.03	12.80	53.80	24.10	80.56	-
7066	1695	1.48	0.88	0.31	1.02	1.25	0.04	0.44	-	-	-	0.10	7.80	51.10	35.50	90.55	-
7070	1685	1.48	1.09	0.30	1.01	1.29	0.03	0.44	-	-	-	0.10	9.00	52.40	32.50	88.52	-
7075	1644	1.20	0.87	0.23	0.92	1.13	0.04	0.43	-	-	-	0.20	12.70	55.30	25.90	84.08	-
7080	1698	1.90	1.00	0.26	1.15	1.16	0.03	0.44	-	-	-	0.10	9.00	52.00	32.30	87.89	-
7201	1652	1.27	0.77	0.24	0.99	1.23	0.06	0.44	-	-	-	0.13	12.90	55.50	25.40	83.73	-

The relationship between the FeO and Ti_2O_3 contents of the titania slags from Table 21 is shown in Figure 20. Also shown is the linear regression line drawn for the data. The data from this study was also compared with the data given by various other authors. This comparison is shown in Figure 21. As expected the data from this study compare very well with that given by Pistorius and Coetsee (2000) for South African slags. The data published by Grau and Poggi (1978), and Pistorius and Coetsee (2000) for the Sorel slags also compare well.

As discussed by Pistorius and Coetsee (2000) it can be seen that the linear regression lines for the Sorel slags lie below that of the South African slags. The reason for this is the higher impurity content of the Sorel slags (Pistorius and Coetsee, 2000). Ban (1988) and Ban et. al. (1988) obtained a semi-logarithmic relationship between the Ti_2O_3 and FeO contents of the slags studied by them. Depending on the FeO content of their slags, the Ti_2O_3 content of their slags is markedly different to those of the other investigators. For example, comparing their data for RBM slags with that of this study and with the data of Pistorius and Coetsee (2000) for South African slags the following comments can be made:

- The equation of Ban et. al. (1988) intersects the linear regression lines of this study and the study of Pistorius and Coetsee (2000) at approximately 8 and 23 per cent FeO.
- At 15 per cent FeO the difference in the Ti_2O_3 content between the respective studies is approximately 6 per cent.
- At values lower than 8 per cent FeO the Ti_2O_3 values diverge sharply and can perhaps be explained in the way the different data sets are fitted.

As explained by Pistorius and Coetsee (2000) high titania slag consists mainly of one solid solution phase, with this phase expected to consist of a mixture of the stoichiometric end members $FeTi_2O_5$ and Ti_3O_5. This should therefore result in a linear relationship between the FeO and Ti_2O_3 content in high titania slags. This FeO-Ti_2O_3 relationship for the $FeTi_2O_5$-Ti_3O_5 tie line is also shown in Figure 21. As found by Pistorius and Coetsee (2000) this line lies well above the other data lines. As explained previously, Pistorius and Coetsee (2000) re-calculated the data in their paper to take into account the effect of the impurities (see equations (VII) and (VIII)). Taking this into account their data correlated very well with the FeO-Ti_2O_3 relationship for the $FeTi_2O_5$-Ti_3O_5 tie line. It should however be pointed out at this stage that the correction applied by Pistorius and Coetsee (2000) for the Al_2O_3 content is not relevant to South African slags (see equation (VIII)). This is due to the low Al_2O_3/SiO_2 ratios found in the glass phases for South African slags. This is typified by the results shown in Table 19, where the molar Al_2O_3/SiO_2 ratios varied between 0.02 and 0.07 for the different glass phases. Due to the low levels of these impurities it does however not have a significant impact on the results.

These calculations were also done for the data in this study, also by using equations (VII) and (VIII), followed by the normalisation of the TiO_2, equivalent FeO and equivalent Ti_2O_3 data to 100 per cent. The results obtained for the re-calculated data are shown in Figure 22. Also shown is the linear regression line for the data, with a R^2 value of 0.75 obtained. This is slightly higher than the R^2 value of 0.70 obtained in Figure 20, indicating that the inclusion of the impurities marginally improves the linear regression fit. The results show that the inclusion of the impurities definitely improves the correlation with the $FeTi_2O_5$-Ti_3O_5 tie line composition relationship, with the linear regression line only slightly below the tie line composition. The reason for the difference can possibly be explained by some oxidation of the Ti^{3+} content of the slag on cooling.

Figure 20: Relationship between the FeO and Ti_2O_3 content of titania slag (This study)

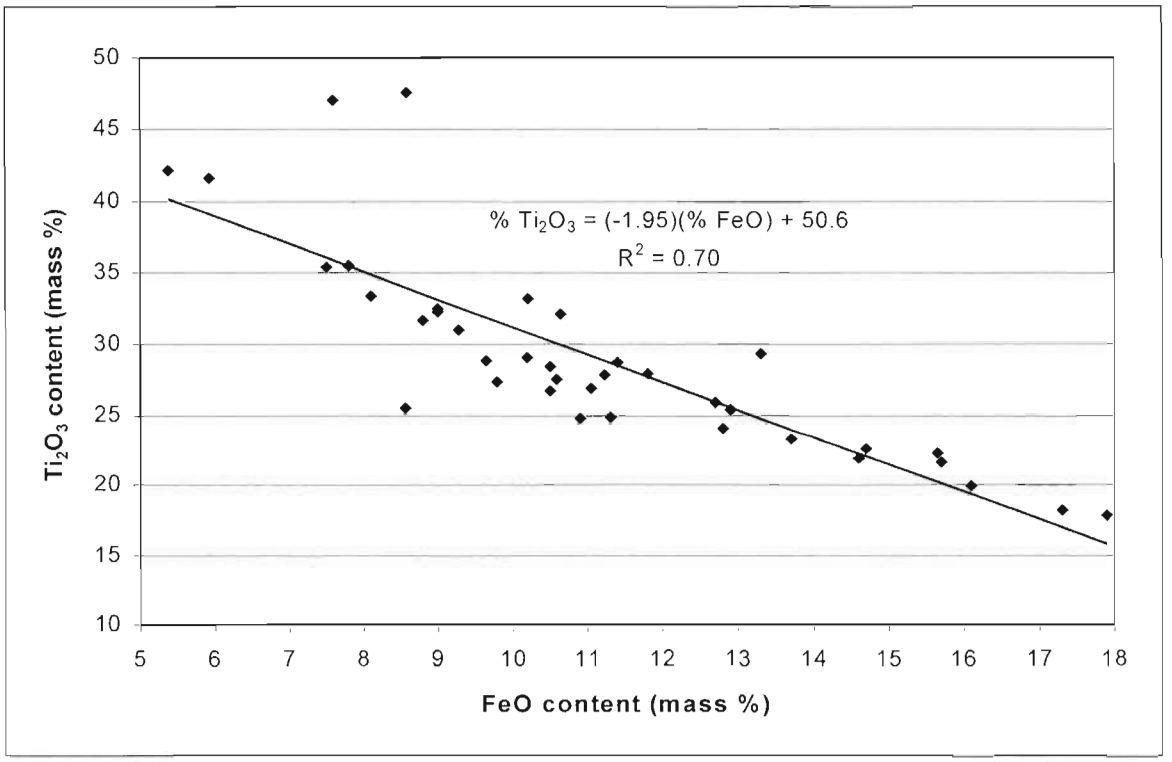

Figure 21 : Comparison of various results for the FeO-Ti_2O_3 relationship in titania slags

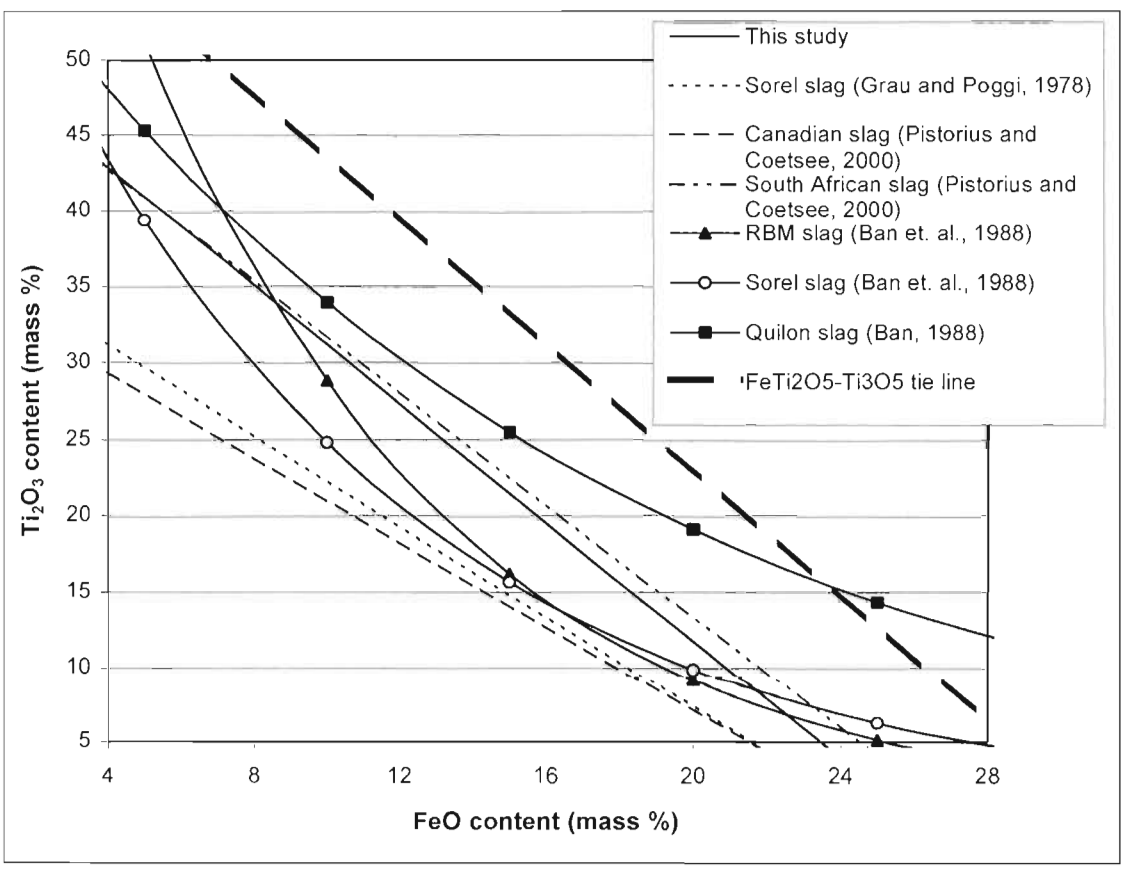

Figure 22: Relationship between the FeO and Ti_2O_3 content of titania slag in this study (Effect of impurities taken into account)

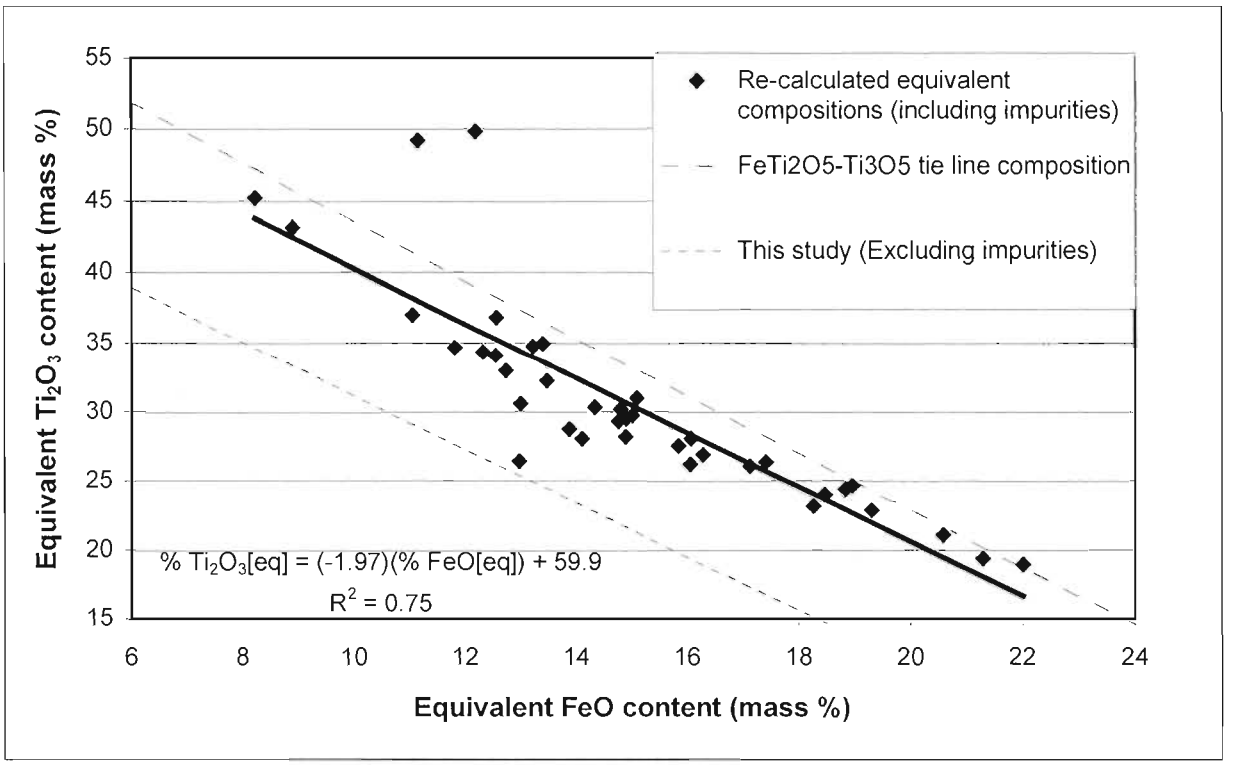

The relationship between the FeO content and the total titanium content of the slag (expressed as TiO_2) was also plotted. This is shown in Figure 23. Also shown is the composition line for the $FeTi_2O_5$-Ti_3O_5 tie line (dashed line). Once again it can be seen that by excluding the impurities in the slag there is a substantial difference between the tie line composition and the linear regression line for the data not including the impurities. The data was re-calculated to include the effect of the impurities. To calculate the equivalent total titanium content expressed as TiO_2 (% TiO_2[eq]), the following equation was used (M_{TiO2} and M_{Ti2O3} the molar mass of the respective compounds):

$$\% TiO_2[eq] = \% TiO_2 + (\% Ti_2O_3[eq])(2M_{TiO2}/M_{Ti2O3}) \ldots(XI)$$

For the calculation of % Ti_2O_3[eq], equation (VIII) was again used. The effect of including the impurities can be seen very clearly in Figure 23. Excellent correlation between the calculated relationship and the tie line composition are observed. This also tends to confirm the earlier contention that the Ti^{3+} content of the slags decreased slightly during the cooling process due to oxidation. The calculated line also has an R^2 value of 0.99, showing the excellent fit of the data. This R^2 value is also substantially higher than the value of 0.75 found for the Ti_2O_3[eq]-FeO[eq] relationship (see Figure 22). The reason for the difference can probably be attributed to the uncertainty involved with the wet chemical technique used for the analysis of the Ti_2O_3 content of the slags.

Figure 23: Relationship between the FeO and total titanium content (expressed as TiO_2) of titania slag in this study

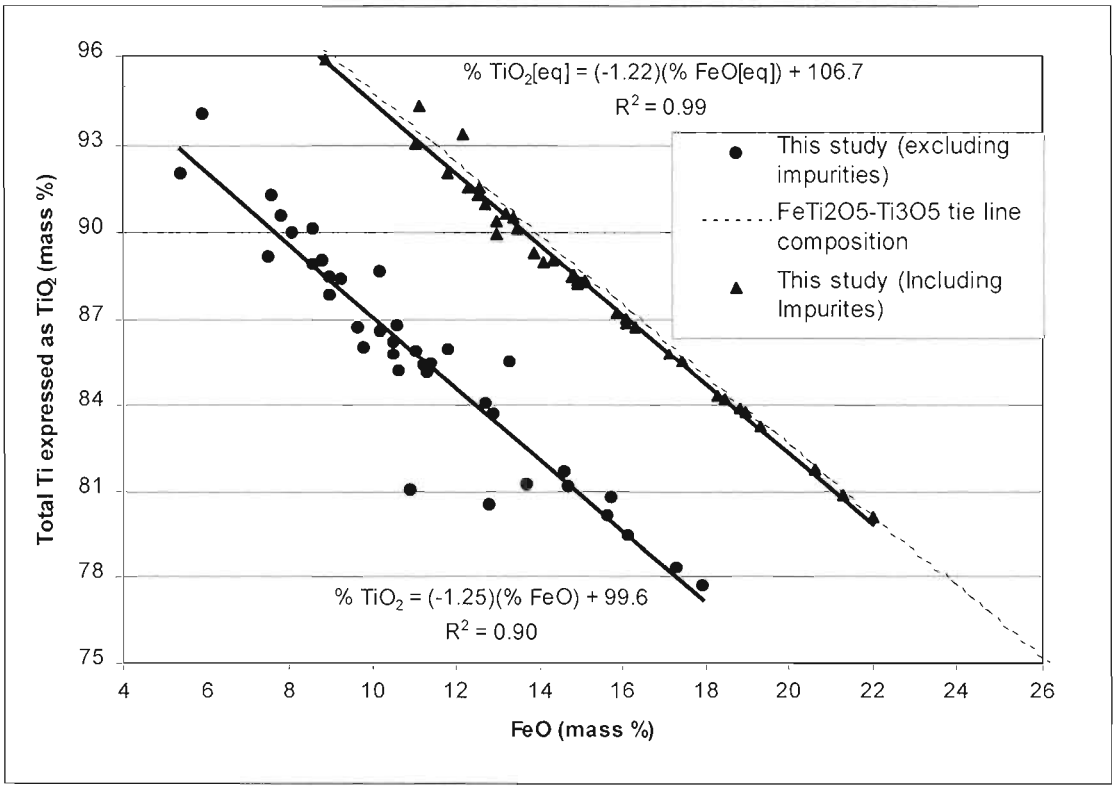

2.4.3 TAPPING TEMPERATURES FOR ILMENITE SMELTING

The tapping temperatures of the various high titania slag samples are also given in Table 21. This tapping temperature data was then plotted on the conjectural $FeTiO_3$-TiO_2-$TiO_{1.5}$ liquidus diagram proposed by Pistorius and Coetsee (2000) as a function of the slag composition. The following equations were used for the calculation of the compositions (n is defined as the number of moles of each species):

$$n(FeO)_{Total} = n(FeO) + n(MgO) + n(MnO) \ldots(XII)$$

$$n(TiO_{1.5})_{Total} = n(TiO_{1.5}) + n(AlO_{1.5}) + n(CrO_{1.5}) + n(VO_{1.5}) \ldots(XIII)$$

$$n(FeTiO_3)_{Total} = n(FeO)_{Total} \ldots(XIV)$$

$$n(TiO_2)_{Residual} = n(TiO_2) - n(FeO)_{Total} \ldots(XV)$$

The total number of moles was then normalised in order to obtain the mole fractions. These equations were used to take into account the effect of the impurities that are part of the slags. The ternary diagram, with the calculated slag compositions, is shown in Figure 24. The tapping temperatures shown in the diagram were divided into the following three temperature regimes:

- Tap temperatures above 1700 °C.
- Tap temperatures between 1700 and 1650 °C.
- Tap temperatures below 1650 °C.

The following comments can be made based on the ternary diagram:

- The bulk of high titania slag consists of the M_3O_5 phase (as illustrated by the Ti_3O_5-$FeTi_2O_5$ tie line). It should therefore be expected that the slag compositions should lie on, or close to this tie line. With an increase in reduction (reducing the FeO content of the slag and increasing the Ti^{3+} content of the slag) the composition of the slag should shift towards the Ti_3O_5 end member. If this diagram is correct it indicates that the liquidus temperature of the slag should increase with an increase in the reduction of the slag.

Figure 24: Tapping temperatures as a function of the slag composition (compositions expressed as mole fractions)

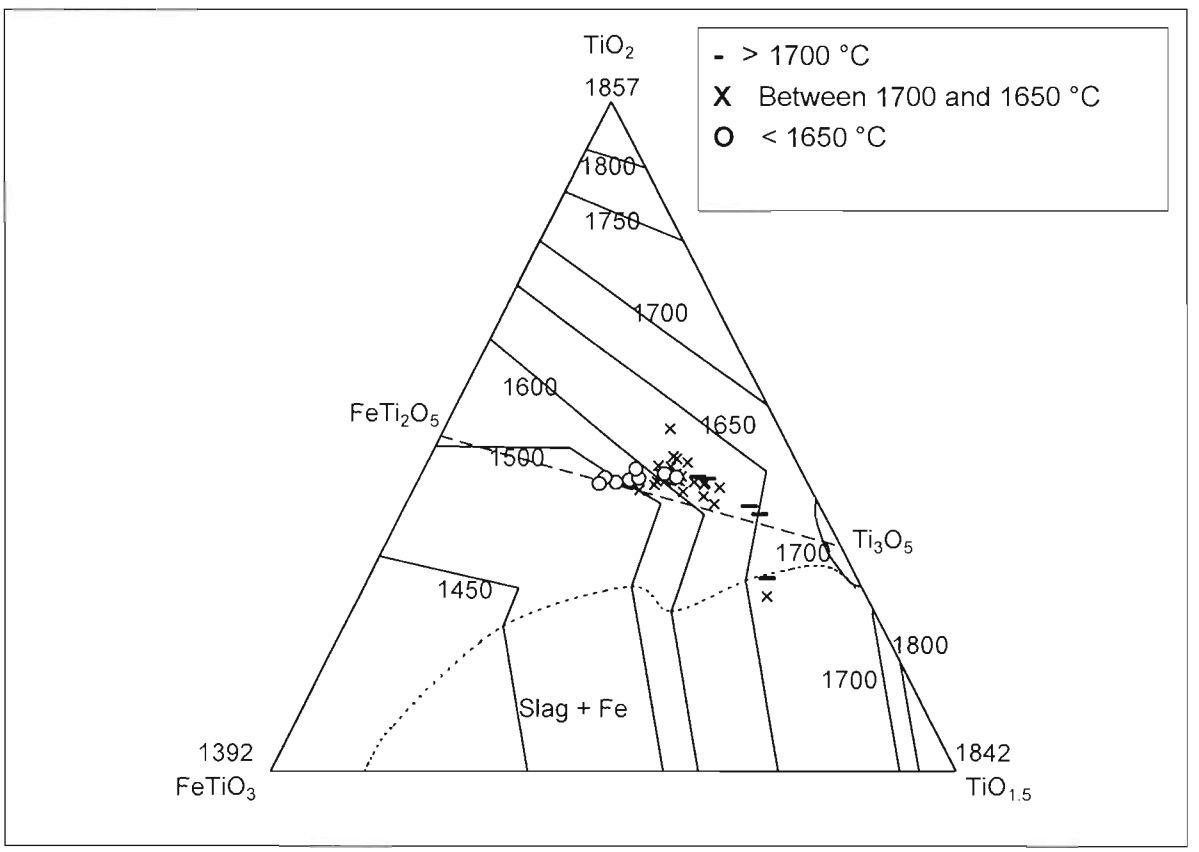

- From the data it can be seen that the tap temperatures above 1700 °C in general are closer to the Ti_3O_5 end member, while the tap temperatures below 1650 °C in general are closer to the $FeTi_2O_5$ end member.
- The data points lie on or above the Ti_3O_5-$FeTi_2O_5$ tie line. This is probably an indication that some of the Ti^{3+} in the slag oxidised on cooling. There are two data points that lie substantially below the Ti_3O_5-$FeTi_2O_5$ tie line (sample numbers 3228 and 3229 from Table 21). The following possible reasons for this can be put forward:
  - It is possible that these compositions were determined incorrectly, as their position in the phase diagram can not be otherwise explained.

- As these two samples contain high levels of Ti_2O_3 it can be postulated that a highly reduced M_2O_3 phase formed. The formation of M_2O_3 phases in high titania slags has previously been suggested by Russian investigators (see Handfield and Charette, 1971).

- In general it seems that the tapping temperatures lie substantially above the proposed liquidus temperatures. For example, all the tapping temperatures between 1650 and 1700 °C (with one exception) are below the 1650 °C temperature isotherm. Some of the tapping temperatures in this range were also plotted close to the 1500 °C isotherm. It therefore seems likely that the difference between the liquidus and tapping temperatures can be ascribed to the "super heat" present in the slags. In general the difference between the liquidus and tap temperatures seems to be between 50 and 100 °C. It should also be emphasised that the tap temperatures are taken in the ladle. In the past it has been found that the temperature in the furnace is somewhat higher (in the order of 20 °C) than the tap temperature. This has however not been quantified in this study.

In Figure 25 the tap temperature of various slags are shown as a function of the FeO content of the slags (data once again from Table 21). A fairly good correlation for this relation was obtained ($R^2 = 0.87$).

Figure 25: Tap temperature of slag as a function of the FeO content of the slag

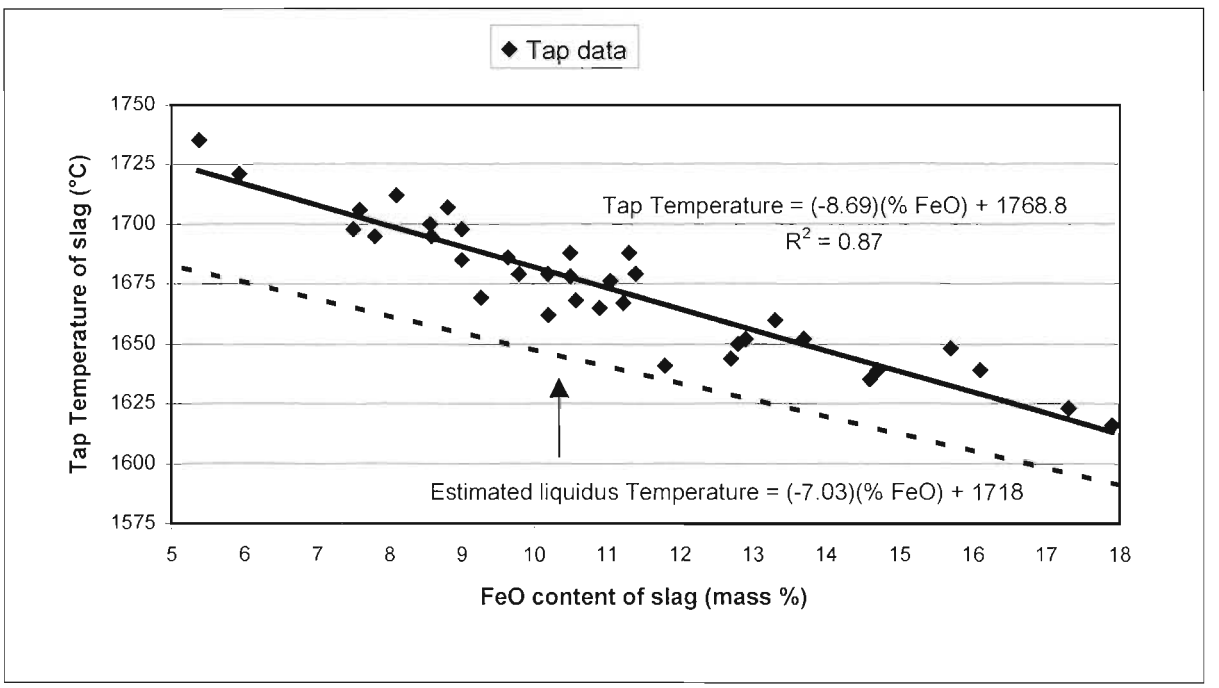

Also shown in Figure 25 is an equation (shown by the dashed line) for the estimated liquidus temperature as a function of the FeO content. Titania slag consists mainly of a M_3O_5 phase with a specific composition, with the composition being defined by the $FeTi_2O_5$ and Ti_3O_5 end members. The liquidus temperatures for these two compositions are available from the data of Eriksson and Pelton (1993) for the FeO-TiO_2 and Ti_2O_3-TiO_2 binary systems. It was assumed that a linear relationship between the liquidus temperatures of these two end members would provide a good estimate of the theoretical liquidus temperatures of the titania slags. The liquidus temperatures for these end members from the relevant phase diagrams are 1500 °C for $FeTi_2O_5$ (31.0 mass per cent FeO; 69 mass per cent TiO_2) and 1718 °C for Ti_3O_5

(64.3 mass per cent Ti_2O_3; 35.7 mass per cent TiO_2). For the calculation of the equation it was assumed that the liquidus temperature for this M_3O_5 tie line (shown schematically in Figure 24) increases linearly from $FeTi_2O_5$ to Ti_3O_5. The effect of impurities on the estimated liquidus line has not been taken into account. For example the liquidus temperature of $MgTi_2O_5$ according to Eriksson and Pelton (1993) is 1657 °C. It can therefore be expected that for slags which contain appreciable amounts of magnesium, that the liquidus temperature would be higher.

It is interesting to note in Figure 25 that the slopes of the estimated liquidus line and the tap temperature line are similar. A slight divergence of the lines takes place as the FeO content of the slags decrease. Assuming that the calculated liquidus temperature equation is correct, it seems that the tap temperature is approximately 25 to 50 °C above the liquidus temperature of the slag that is estimated in this way.

In Figure 26 the tap temperature of the slag is shown as function of the Ti_2O_3 content of the slag. This data shows more scatter than the data for Figure 25 (R^2 = 0.62). This is probably due to the quality of the analytical techniques used for the two components. FeO is analysed by using an accurate instrumental technique such as ICP or XRF, while the Ti_2O_3 content of the slags is determined by a more difficult wet chemistry technique.

Figure 26: Tap temperature of slag as a function of the Ti_2O_3 content

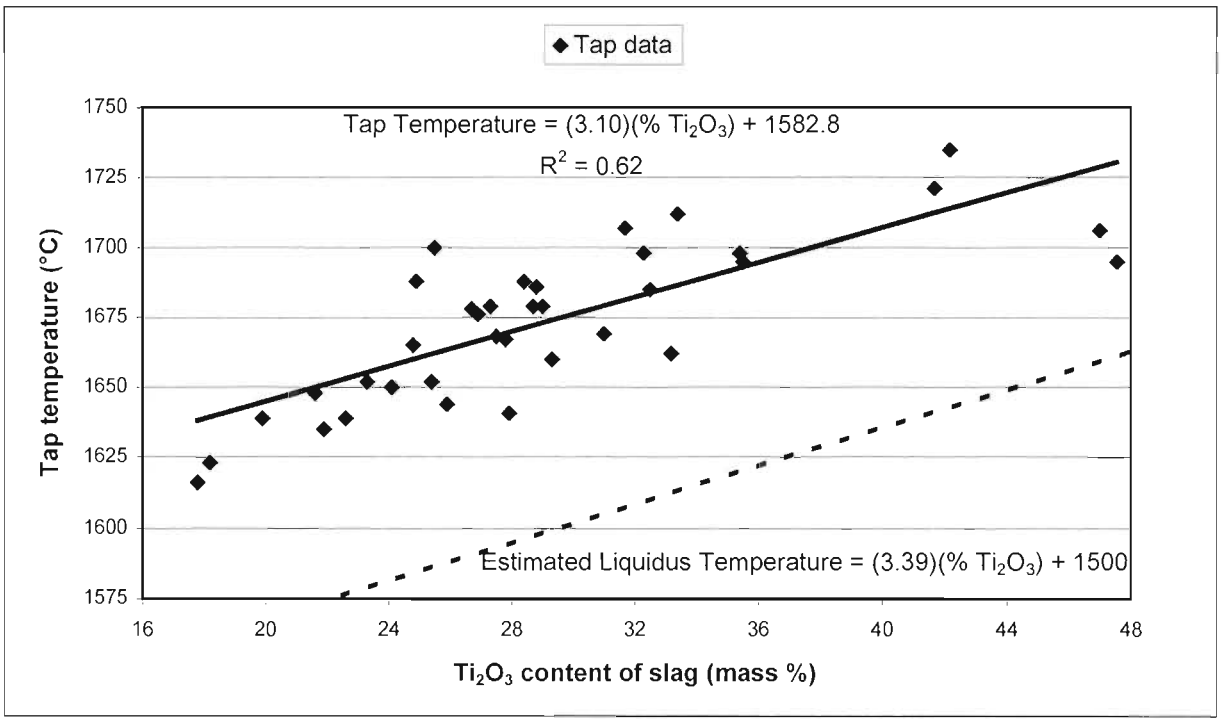

The estimated liquidus temperature is shown as a function of the Ti_2O_3 (dashed line). This was again calculated by using the liquidus temperature data for $FeTi_2O_5$ and Ti_3O_5. According to Figure 26 it seems that the tap temperature is approximately 75 °C higher than the liquidus temperature of the slag, once again assuming that the calculated liquidus temperature relationship is correct.

To investigate the relevance of using a linear liquidus temperature relationship for the $FeTi_2O_5$-Ti_3O_5 tie line, Figure 27 was constructed. For this purpose the data from Pesl and the data from Pistorius and Coetsee were compared with the linear temperature relationship. In each instance the liquidus temperature data for $FeTi_2O_5$ and Ti_3O_5 from Eriksson and Pelton was assumed to be correct. Figure 27 shows that up to a Ti_3O_5 mole fraction of approximately 0.4 (that is approximately 19 mass per cent FeO), very little change in the liquidus temperature is predicted. The figure shows that from a Ti_3O_5 mole fraction of approximately 0.6 (approximately 13 mass per cent FeO), a fairly good correlation is obtained.

Figure 27: Liquidus temperature data for the $FeTi_2O_5$-Ti_3O_5 tie line

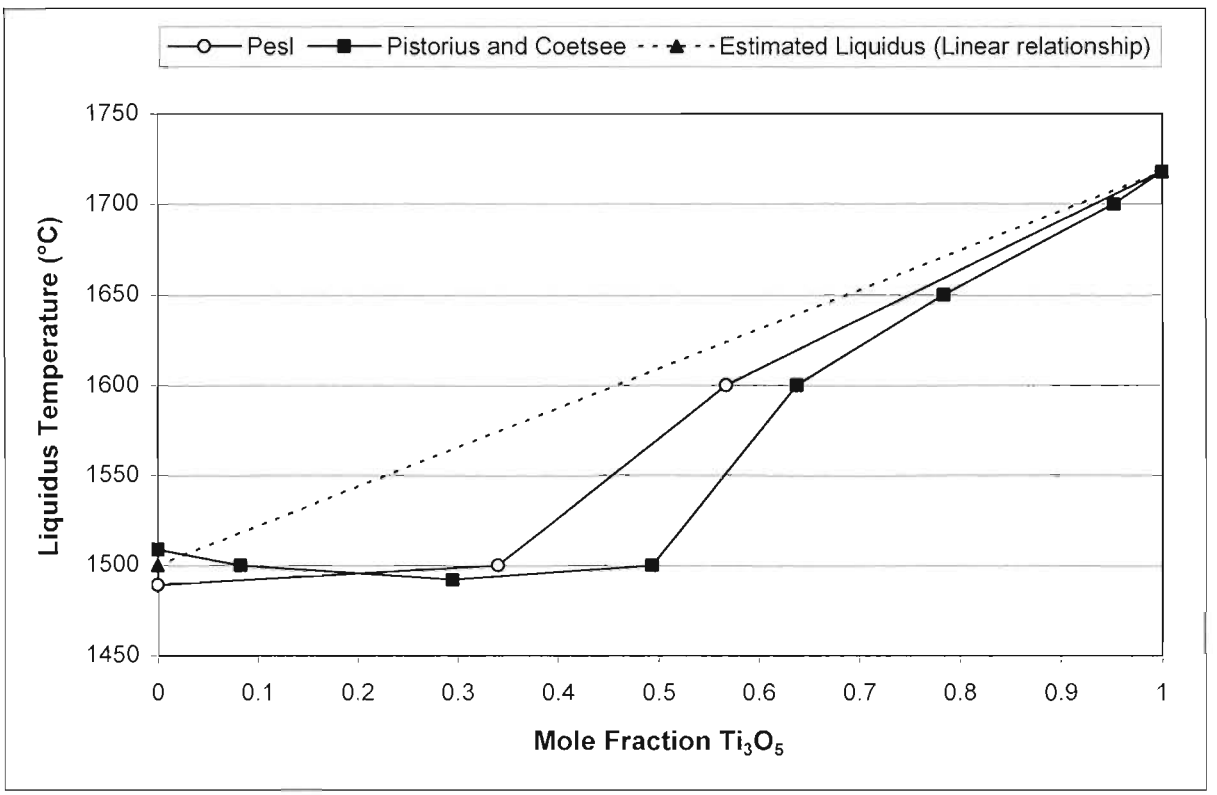

2.5 CONCLUSIONS AND RECOMMENDATIONS

High titania slags consist mainly of a M_3O_5 solid solution phase. In the Fe-Ti-O system this solid solution is continuous only at temperatures above approximately 1350 °C. The M_3O_5 phases found in the spoon samples are therefore only metastable at room temperature. The M_3O_5 phases consist of an orthorhombic, pseudobrookite structure (AB_2O_5). The unit cell contains 4 atoms on the A site, 8 atoms on the B site and 20 oxygen atoms. Mössbauer spectroscopy results shows that the majority of iron is found in the larger A site. The oxidation state of iron in these slags was also confirmed to be +2.

Neutron diffraction studies can also be employed in future to clarify the distribution of iron and titanium in the M_3O_5 structure. The electron densities of iron and titanium are sufficiently similar so that X-ray diffraction cannot always distinguish between them. The scattering cross-section of iron for neutrons is however three times that of titanium and of the opposite sign (Lindsley, 1976).

Two types of glass phases were also found in the high titania slags. These phases consist mainly of SiO_2. The difference between the two types of phases is with regard to the presence of impurities, as well as the levels of these impurities. Reeves and Reeves (1997) mention that the behaviour of silica during the subsequent chlorination process is not understood. It could therefore be worthwhile if the chlorination behaviour of these types of glass phases were studied in future.

Of interest also was the presence of fine metallic precipitates (less than approximately 3 μm) in rutile crystals. It has been suggested that these phases form due to the reaction of Ti_2O_3 and FeO in the slag to form rutile and the metallic iron (Toromanoff and Habashi, 1984). The conditions under which this reaction occurs could also be an area for further study.

Results on the FeO and Ti_2O_3 relationships in the titania slags closely follows the composition of the $FeTi_2O_5$-Ti_3O_5 tie line (as found by Pistorius and Coetsee, 2000). It is also suggested that the tapping temperatures have a "superheat" of approximately 50 °C over the proposed liquidus temperatures. An area of further study could be the determination of the liquidus temperatures along the $FeTi_2O_5$-Ti_3O_5 tie line.